Freeze/thaw cycles and rain-on-snow

Structure of this lecture

1. What is freeze/thaw and why are we interested in it?
2. Sensors, data and algorithms
3. Applications with focus on events (esp. rain-on-snow)

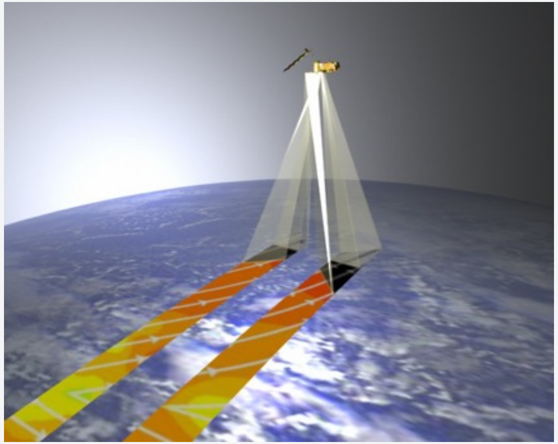

© ESA - AOES Medialab

What is freeze/thaw and why are we interested in it?

- Temperature change which results in change of physical properties
- Assumption presence of water
- High dynamics – diurnal variations common, minimum daily sampling required

- Monitoring of landsurface
  - Changes type throughout the season
  - We need to consider snow and/or soils

What is freeze/thaw and why are we interested in it?

- Temperature change which results in change of physical properties
- Assumption presence of water
- High dynamics – diurnal variations common, minimum daily sampling required

- Relevant for e.g.
  - Soil processes, e.g. microbial activity → carbon cycle
  - Snow properties of relevance for subsoil temperatures → permafrost
  - Changes in snow structure → wild life

Where does freeze/thaw occur?

- Often freeze/thaw is asscoiated with permafrost – actually only characterizes the state of the top of the active layer, by definition not permafrost

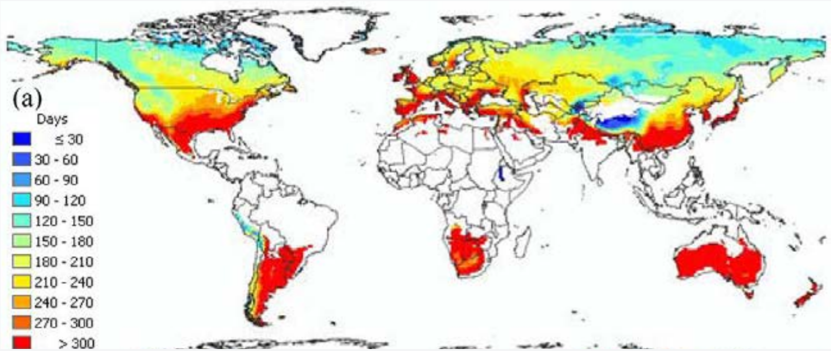

Number of unfrozen days, Kim et al. 2011

Which sensors are used?

- Thermal: Landsurface temperature records require gap filling
- Microwave range primarily used
  - No problem with clouds & illumination
  - Sensitivity to freeze/thaw
  - High sampling rate with coarse spatial resolution

- Scatterometer (C-band, 5.3; Ku-band 13.4 GHz), C-band SAR experimentally
- Radiometer (1.4, 19, 37 GHz)

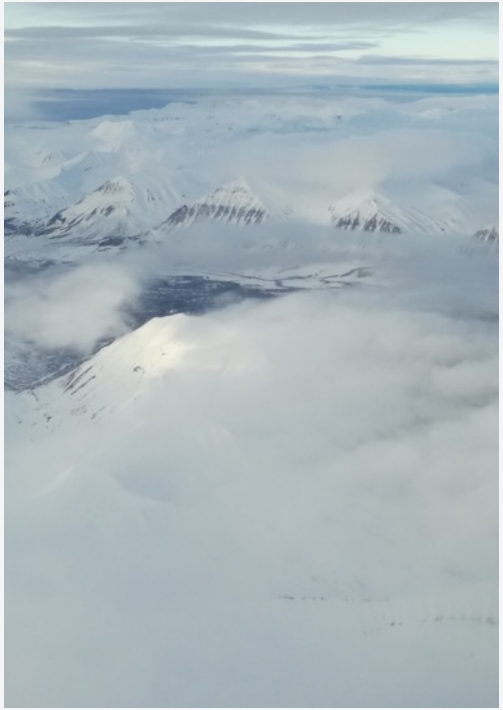

Example Metop ASCAT 5.3 GHz, since 2007 (Metop A, B …)

Figa et al. 2002

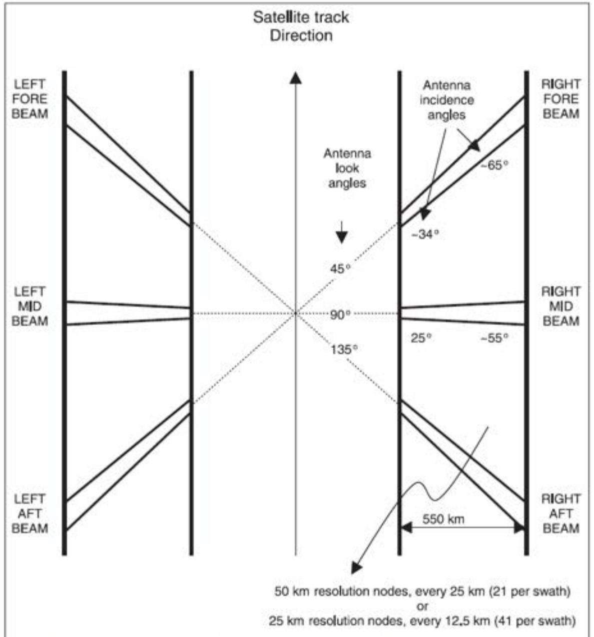

Figure 2. ASCAT swath geometry. Dimensions are given for the right swath, and the left swath is symmetric with respect to the satellite ground track.

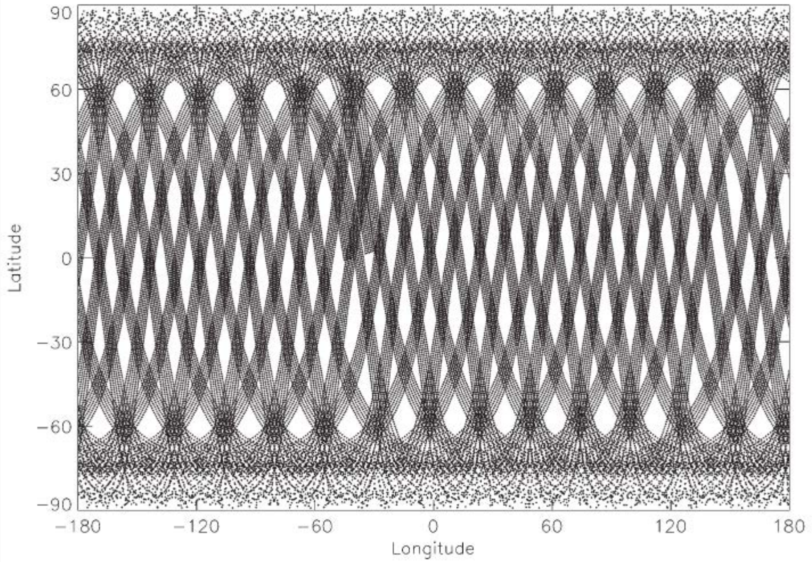

Figure 1. ASCAT coverage for 1 day. The swath coverage has been simulated by resolving the across-track viewing geometry, considering the nominal MetOp orbit of a 29 day (412 orbits) repeat cycle with ascending node at 21:30 and a minimum orbit height of 822 km.

Daily coverage

Example Seawinds on QuikScat 13.4 GHz, 1999 - 2009

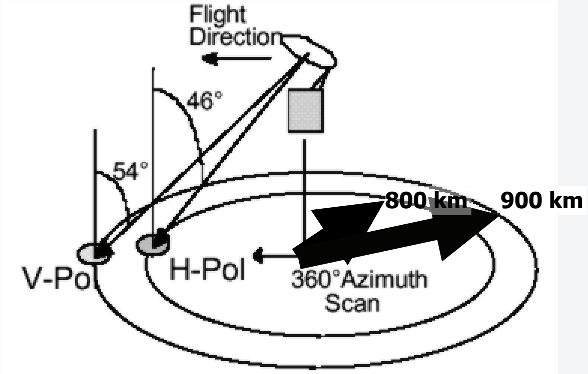

Perry 2000

Distribution of footprints and their time stamp

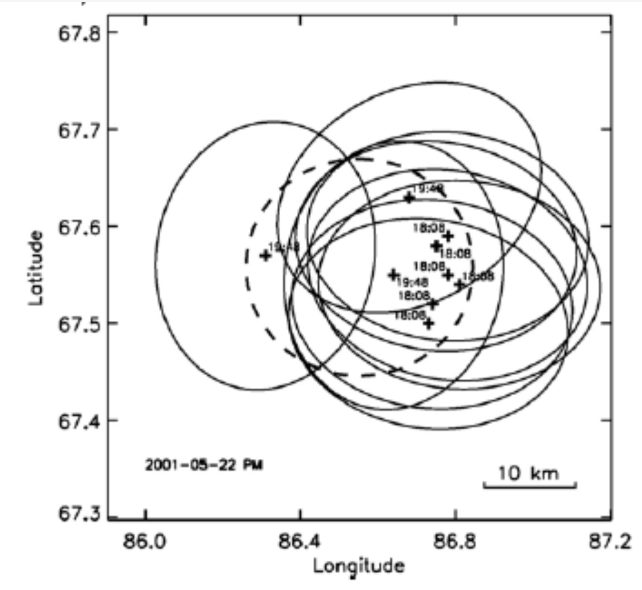

Bartsch, A., Kidd, R., Wagner, W. and Z. Bartalis (2007): Temporal and spatial variability of the beginning and end of daily spring freeze/thaw cycles derived from scatterometer data. Remote Sensing of Environment, 106(3), 360-374

Daily coverage

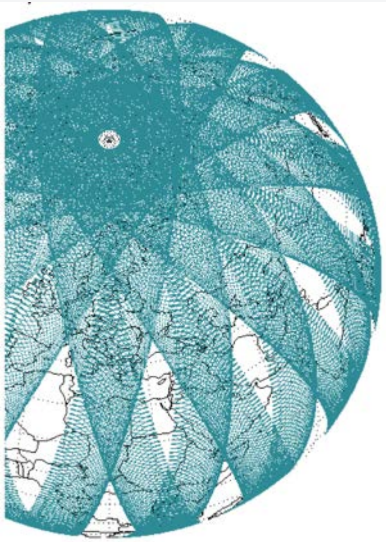

Example SSM/I   19, 37 GHz, 1987 -

Schlüssel (1996)

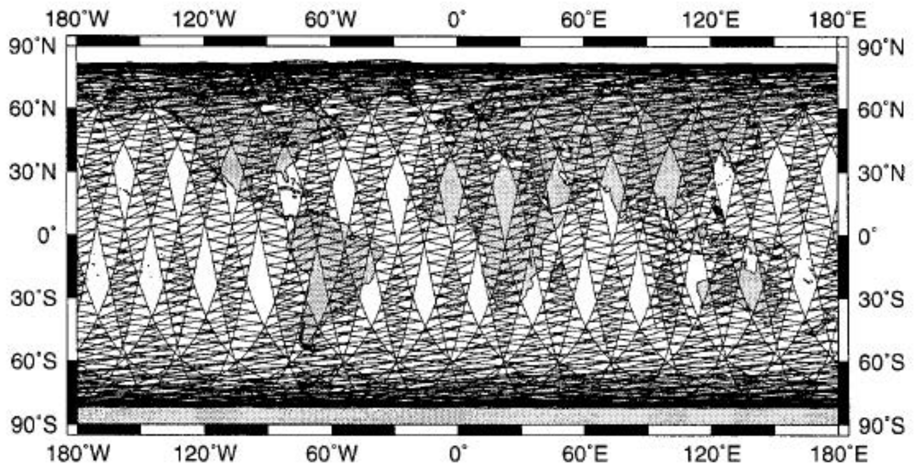

Figure 2.2 Daily coverage of the Earth by the Special Sensor Microwave/Imager.

extension to 1979 possible with SSMR

Algorithms transferable to AMSRE and AMSR2

Example SMOS and SMAP with 1.4GHz

SMOS

Soil Moisture and Ocean Salinity

MIRAS (Microwave Imaging Radiometer with Aperture Synthesis)

ESA

Launched on November 2nd 2009

SMAP

Soil Moisture *Active* and Passive

NASA

Launched on January 31, 2015

V and H polarization

resolution ~40 km

Global coverage in 3 days

Physical basis

Source: Ulaby & Long (2015)

also need to consider snow

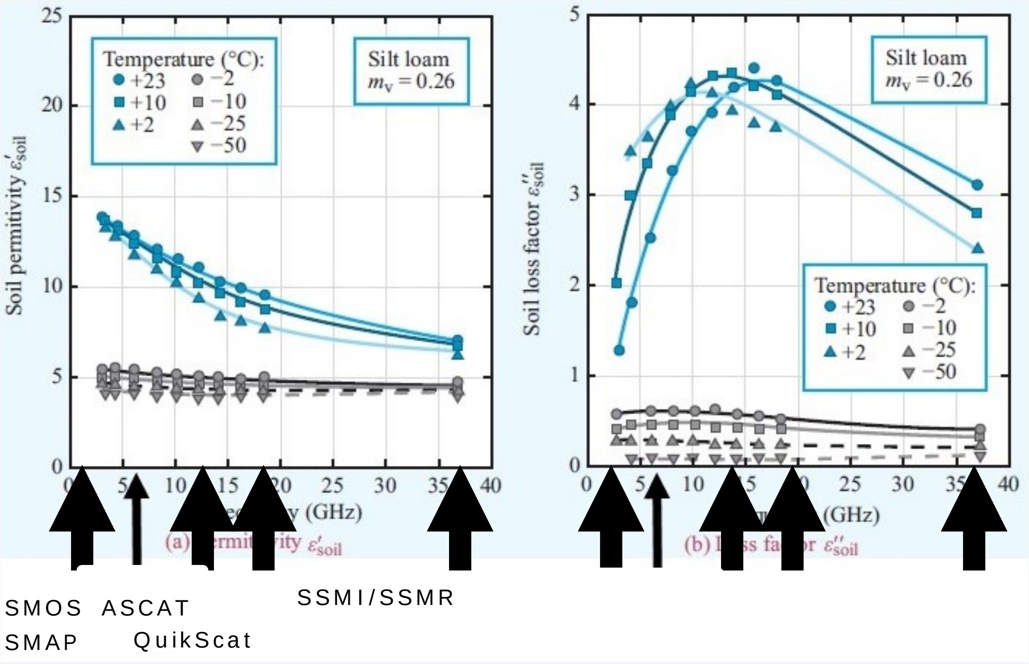

Snow interactions - radar

- Shorter wavelengths such as Ku-band interact with the snow particels
- Longer wavelengths penetrate dry snow and interact with the soil
- Interaction with ice layer at C-band

Dry snow, e.g.

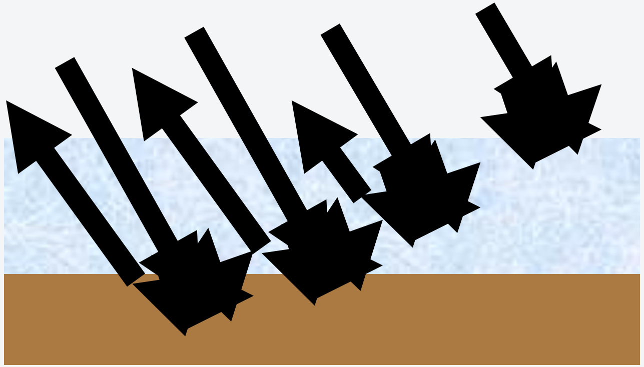

Snow structure and wavelength crucial

(arrows do not represent magnitude, just symbolize interaction)

Example record ASCAT versus QuikScat

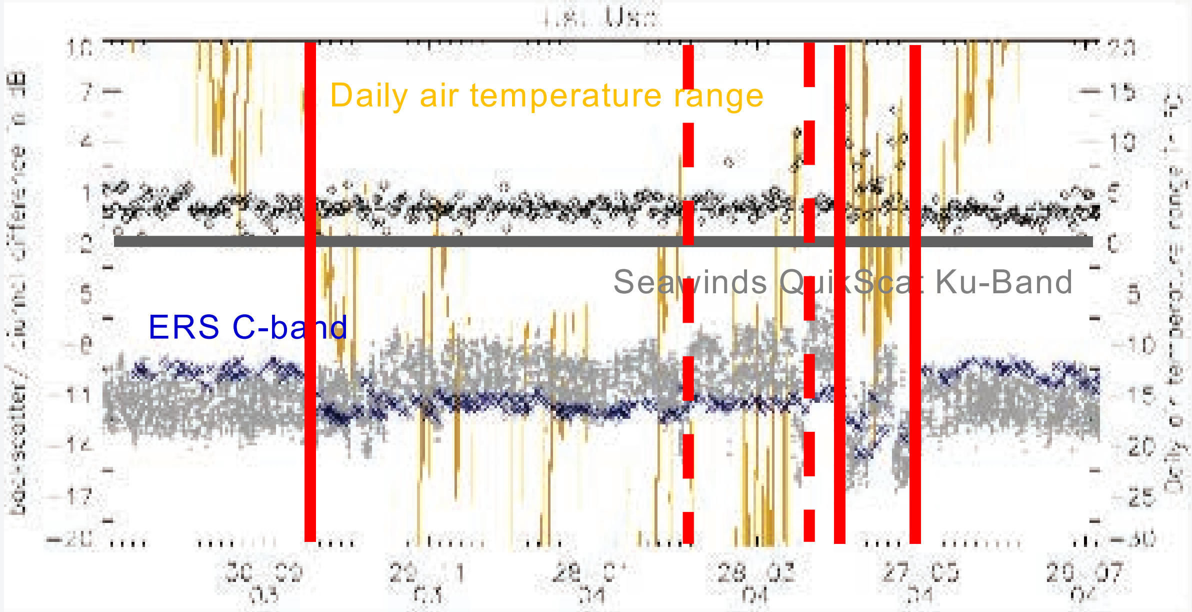

Typical backscatter time series (in dB) for C-Band (blue crosses, source: ERS) and Ku-band (grey points, source: QuikScat) at Ust Usa (56.92 E, 65.97 N) for August 2003 to July 2004. Daily air temperature range in C extracted from the WMO512 dataset is shown as yellow bars. Diamonds represent Ku-band diurnal backscatter difference in dB (source: Bartsch 2010)

Methods and parameters of snow products (excluding glacier and sea ice) from spaceborne scatterometers, status 2010

Reference	Sensor	Method	Parameters
Boehnke & Wismann 1996	ERS (C-band)	Location specific summer (July) and winter (February) backscatter	Thaw timing
Frolking et al. 1999	NSCAT	Five day average backscatter and location specific difference from overall mean	Thaw timing
Kimball et al. 2001	NSCAT	Application of similar method as in Boehnke et al. 1996	Thaw timing
Kidd et al. 2003, Bartsch et al. 2007	SeaWinds QuikSCAT	Diurnal differences with respect to noise and multiple thaw periods	Start and end of major thaw period
Kimball et al. 2004a	NSCAT	Extension of Frolking et al. 1999	Start, end, primary thaw date
Kimball et al. 2004b	SeaWinds QuikSCAT	As in Kimball et al. 2004a	Start, end, primary thaw date plus autumn refreeze
Brown et al. 2007	SeaWinds QuikSCAT	Fixed threshold for deviation from winter (February) backscatter level	Thaw timing
Wang et al. 2008	SeaWinds QuikSCAT	Application of method from Frolking et al. 1999 to average evening backscatter with respect to summer mean values (August)	Snow-off date
Bartsch et al. 2010	SeaWinds QuikSCAT	Moving window with fixed threshold	Refreeze events
Naeimi et al. 2012	Metop ASCAT	Edge detection and location specific threshold from inflection point of temperature function	Surface status +- 1 month of average spring/autumn transition

Bartsch, A. 2010: *Ten years of SeaWinds on QuikSCAT for snow applications*. Remote Sensing 04, 2(4).

C-band time series example

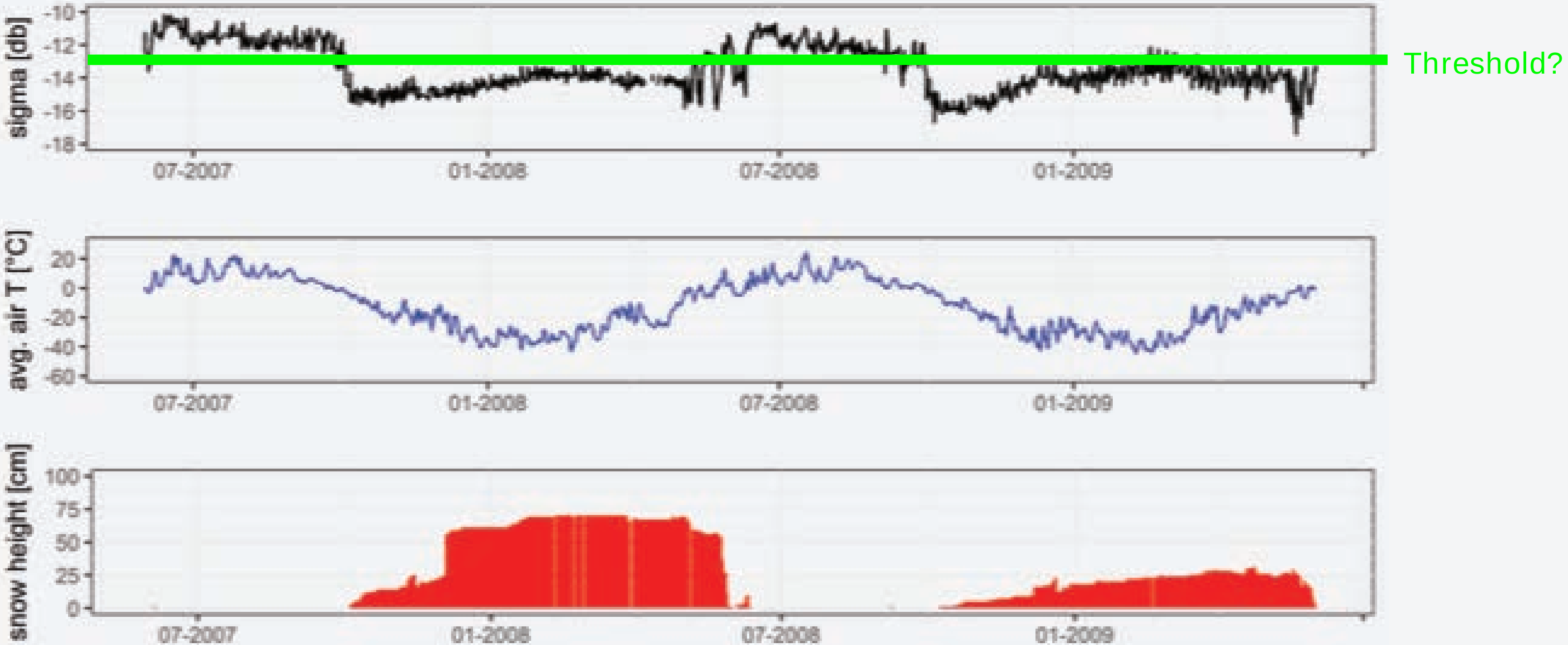

Advanced Scatterometer (ASCAT) backscatter (dB), air temperature (° C) and snow depth (cm) for the World Meteorological Organization (WMO) station Chokurdah Nr. 21946 (70.617, 147.883).

Helena Bergstedt, Simon Zwieback, Annett Bartsch, Marina Leibman: Dependence of C-Band Backscatter on Ground Temperature, Air Temperature and Snow Depth in Arctic Permafrost Regions. Remote Sensing 01/2018; 10(1).

C-band – relationship with ground temperatures

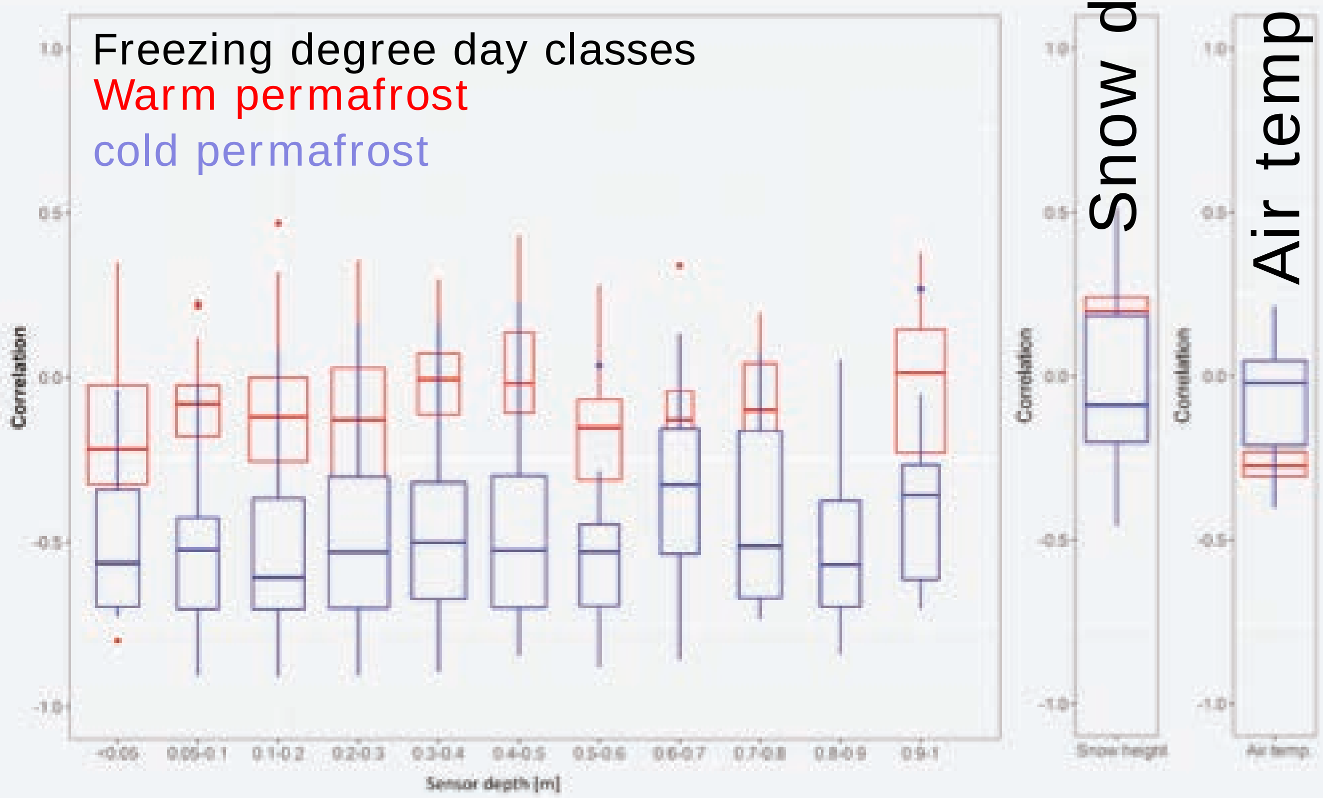

Helena Bergstedt, Simon Zwieback, Annett Bartsch, Marina Leibman: Dependence of C-Band Backscatter on Ground Temperature, Air Temperature and Snow Depth in Arctic Permafrost Regions. Remote Sensing 01/2018; 10(1).

Example ENVISAT ASAR Global monitoring mode

1km, background mode, C-band

Threshold?

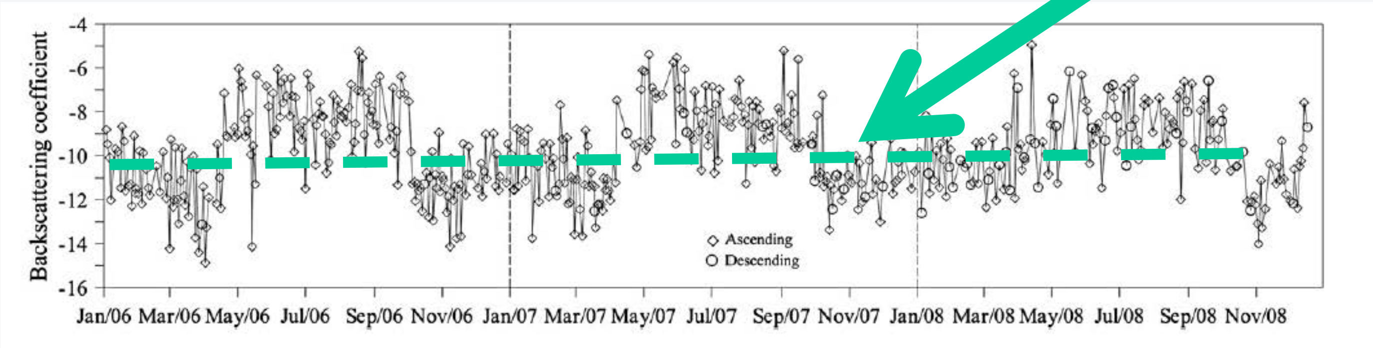

Fig. 3. An example of GM backscatter time-series for a grid point in the study site.

Sang-Eun Park, Annett Bartsch, Daniel Sabel, Wolfgang Wagner, Vahid Naeimi, Yoshio Yamaguchi: *Monitoring freeze/thaw cycles using ENVISAT ASAR Global Mode*. Remote Sensing of Environment 12/2011; 115(12).

austrian polar research institute

Example ENVISAT ASAR Global monitoring mode

Acquired when no other mode requested

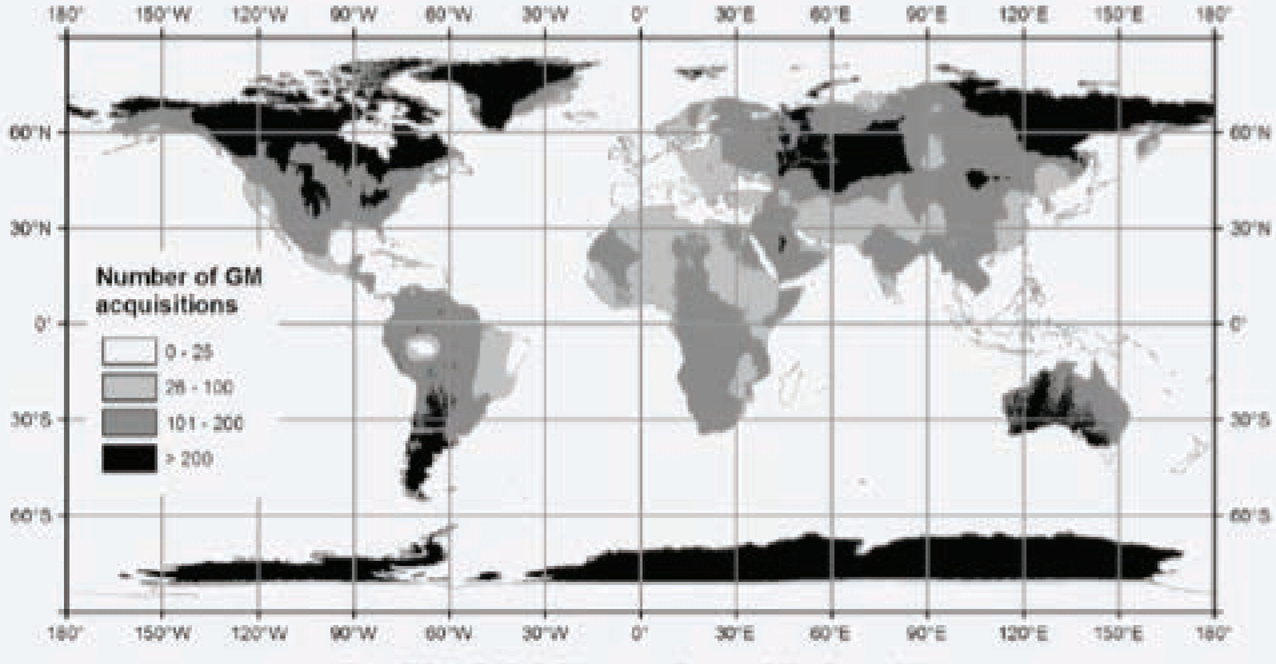

Fig. 1. ENVISAT ASAR GM coverage December 2004–October 2006.

Bartsch et al. 2009, Journal of Environmental Management

A Bartsch, W Wagner, K Scipal, C Pathe, D Sabel, P Wolski: *Global monitoring of wetlands — the value of ENVISAT ASAR global mode*. Journal of Environmental Management 04/2008; 90(7):2226-33.

austrian polar research institute

b.geos

Example ENVISAT ASAR Global monitoring mode

Edge detection – step function, does not allow to detect single freeze/thaw events

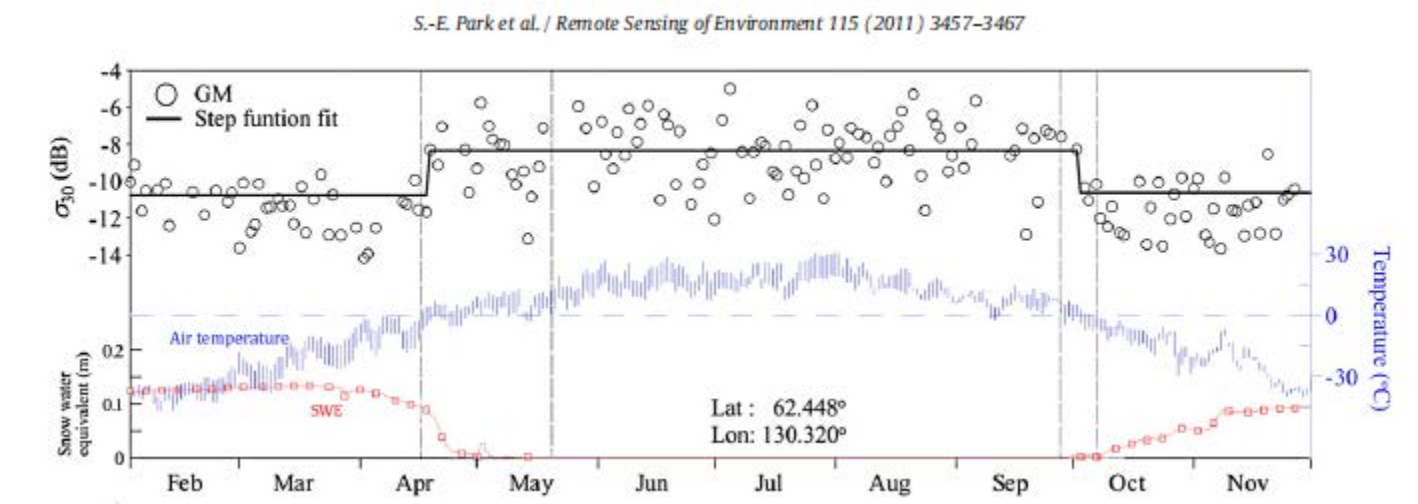

Sang-Eun Park, Annett Bartsch, Daniel Sabel, Wolfgang Wagner, Vahid Naeimi, Yoshio Yamaguchi: *Monitoring freeze/thaw cycles using ENVISAT ASAR Global Mode*. Remote Sensing of Environment 12/2011; 115(12).

Step function applied to Metop ASCAT – transition timing

Thaw

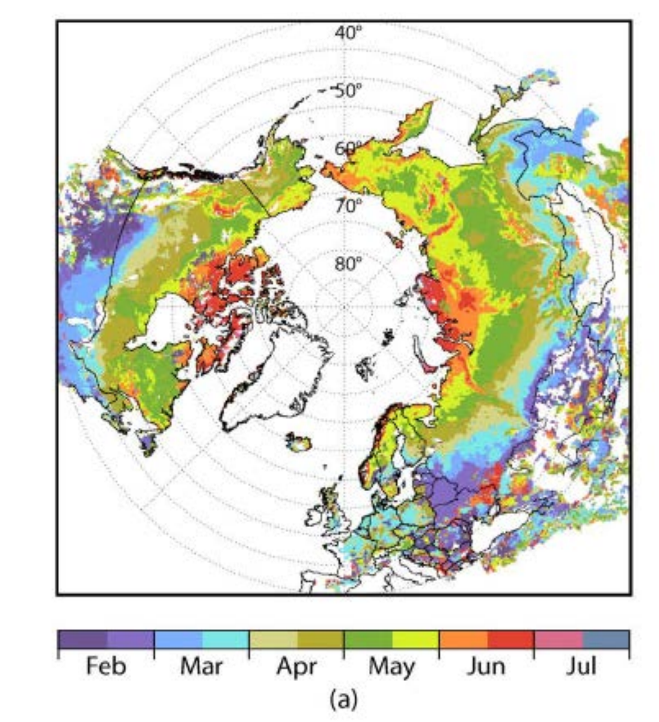

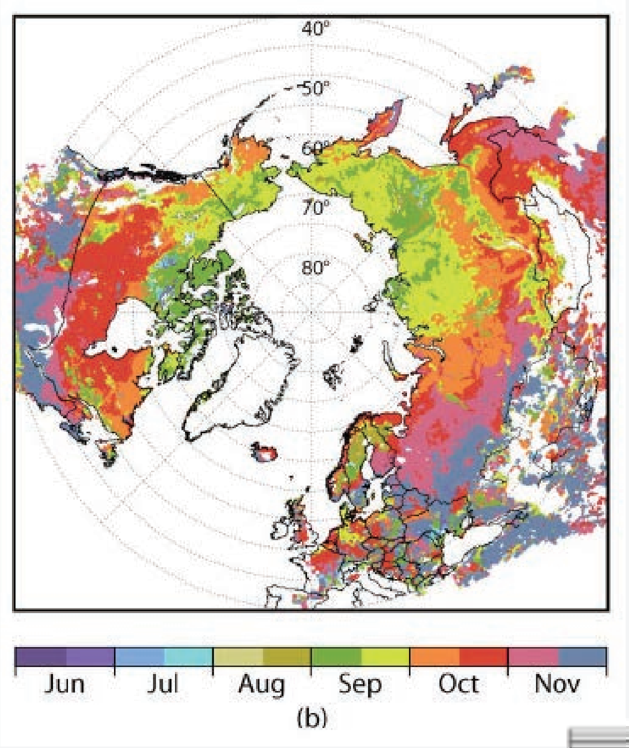

Freeze-up

Naeimi, V., Paulik, C., Bartsch, A., Wagner, W., Kidd, R. Park, S.-E., Elger, K., Boike, J. 2012: *ASCAT Surface State Flag (SSF): Extracting Infor-mation on Surface Freeze/Thaw Conditions from Backscatter Data Using an Empirical Threshold-Analysis Algorithm*. IEEE TGRS 50(7): 2566

austrian polar research institute

Freeze/thaw events from Metop ASCAT

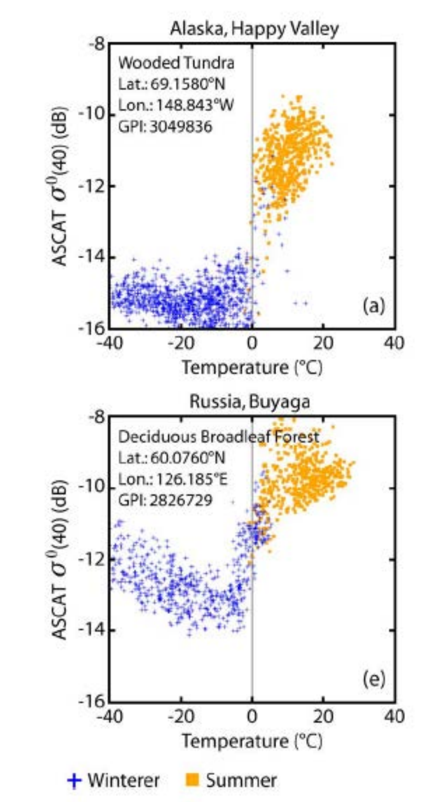

- Reanalyses temperature data for location specific determination of logistic function

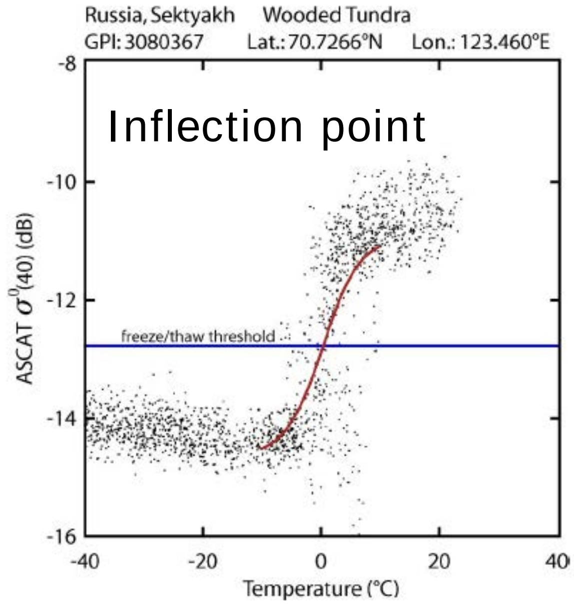

Fig. 4. ASCAT normalized backscatter versus temperature in a grid point near to Sektyakh meteorological station in Russia. Red curve indicates the best logistic function fitted to the measurements. Blue line shows the inflection point of the logistic curve which is assumed as backscatter level at freeze/thaw point.

Naeimi, V., Paulik, C., Bartsch, A., Wagner, W., Kidd, R. Park, S.-E., Elger, K., Boike, J. 2012: *ASCAT Surface State Flag (SSF): Extracting Information on Surface Freeze/Thaw Conditions from Backscatter Data Using an Empirical Threshold-Analysis Algorithm*. IEEE TGRS 50(7): 2566

austrian polar research institute

C-band location specific threshold

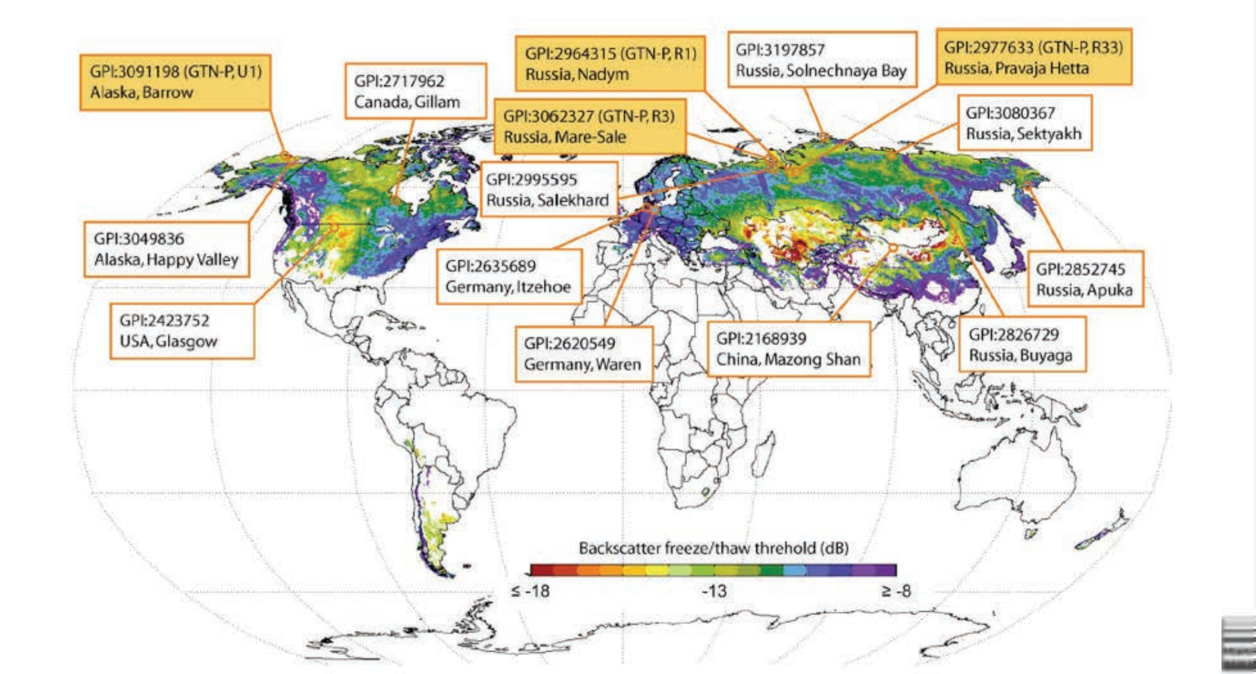

Fig. 5. Global map of backscatter freeze/thaw level showing areas where the SSF method is applicable. Highlighted locations are the grid points shown in other figures throughout the paper.

Naeimi, V., Paulik, C., Bartsch, A., Wagner, W., Kidd, R. Park, S.-E., Elger, K., Boike, J. 2012: *ASCAT Surface State Flag (SSF): Extracting Information on Surface Freeze/Thaw Conditions from Backscatter Data Using an Empirical Threshold-Analysis Algorithm*. IEEE TGRS 50(7): 2566

Comparison ASCAT and ASAR GM

thaw

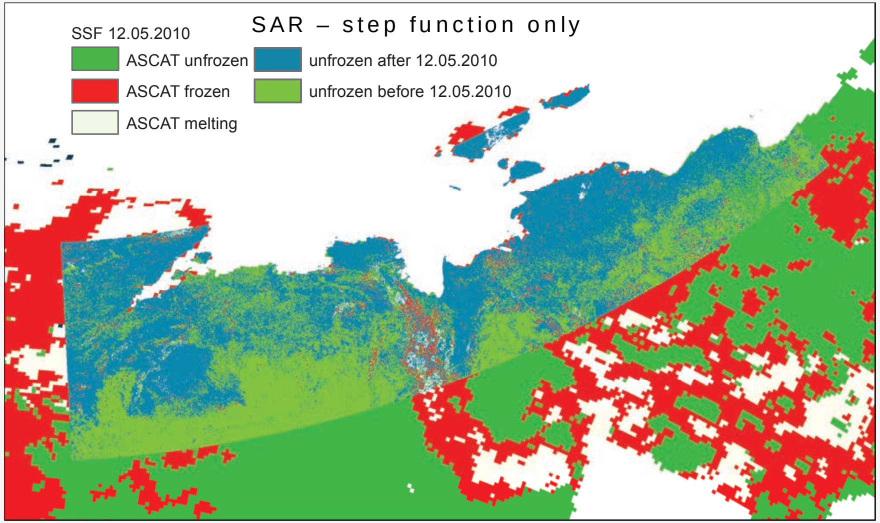

Freeze-up

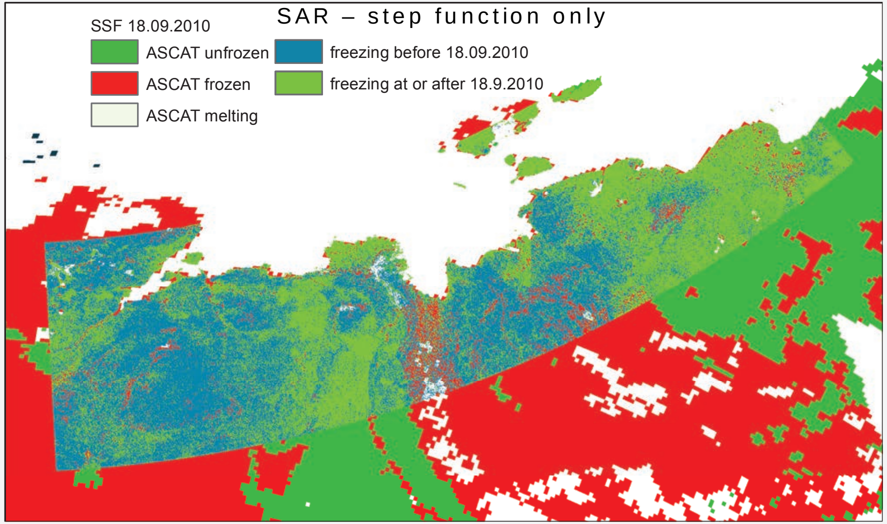

C. Paulik, A. Bartsch, D. Sabel, W. Wagner, C. Duguay, A. Soliman: *Intercomparison of active microwave derived surface status and MODIS land surface temperature at high latitudes*. Proceedings of 2012 IEEE International Geoscience & Remote Sensing Symposium; 07/2012

austrian polar research institute

Comparison ASCAT and ASAR GM

- Daily maps from ASAR GM for 25x25km area

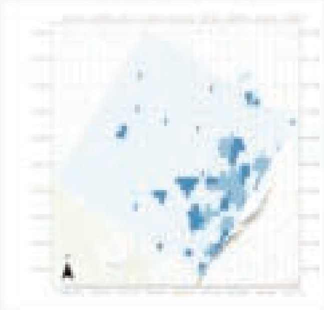

Day 1

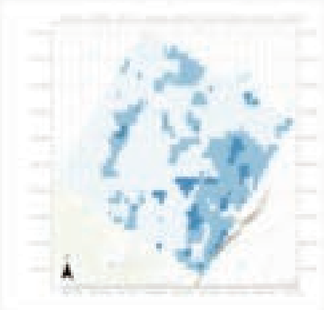

Day 2

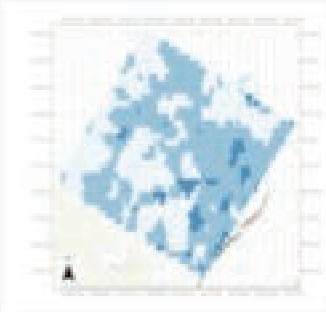

Day 3

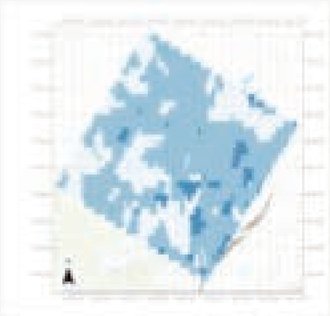

Day 4

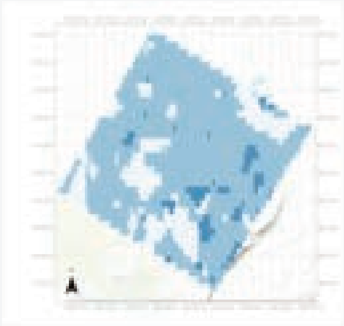

Day 5

- Dependance on topography and landcover

Images courtesy of H. Bergstedt

Comparison ASCAT and ASAR GM

- Tundra

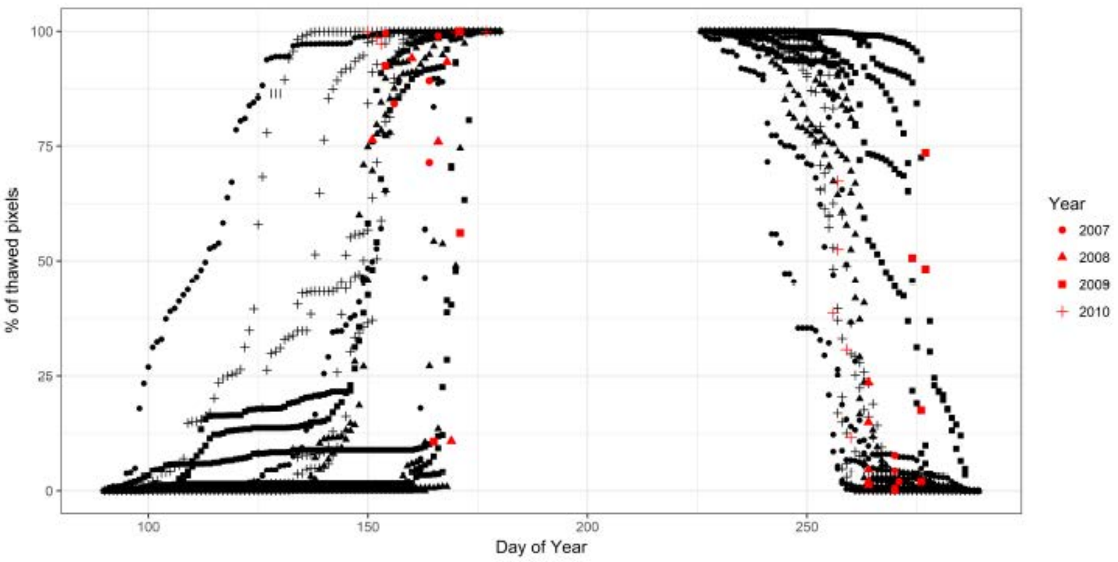

Figure 10. Percentage of thawed SAR pixel within one ASCAT grid cell during transitional periods (indicated by the DOY), including DOY of the last surface state change in the ASCAT product (red symbols) for the selected grid cells with the assigned landscape type Tundra (Laptev Sea 1, Laptev Sea 2, Laptev Sea 3, Laptev Sea 4, Laptev Sea 5), for the ASCAT [42] and SAR [42] datasets.

Helena Bergstedt, Annett Bartsch: Surface State across Scales; Temporal and Spatial Patterns in Land Surface Freeze/Thaw Dynamics. Geosciences (Switzerland) 08/2017; 7(3):65.

Comparison ASCAT and ASAR GM

- Lake dominated tundra

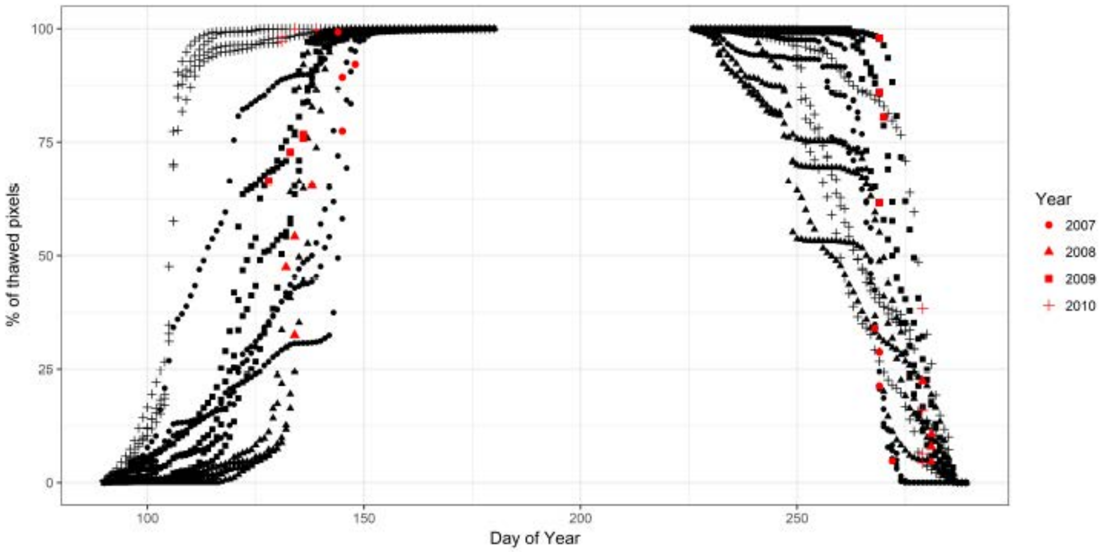

Figure 9. Percentage of thawed SAR pixel within one ASCAT grid cell during transitional periods (indicated by the DOY), including DOY of the last surface state change in the ASCAT product (red symbols) for the selected grid cells with the assigned landscape type Lake dominated tundra (Mackenzie 1, Mackenzie 2, Mackenzie 3, Mackenzie 4), for the ASCAT [42] and SAR [42] datasets.

Helena Bergstedt, Annett Bartsch: Surface State across Scales; Temporal and Spatial Patterns in Land Surface Freeze/Thaw Dynamics. Geosciences (Switzerland) 08/2017; 7(3):65.

Comparison ASCAT and ASAR GM

- Forest

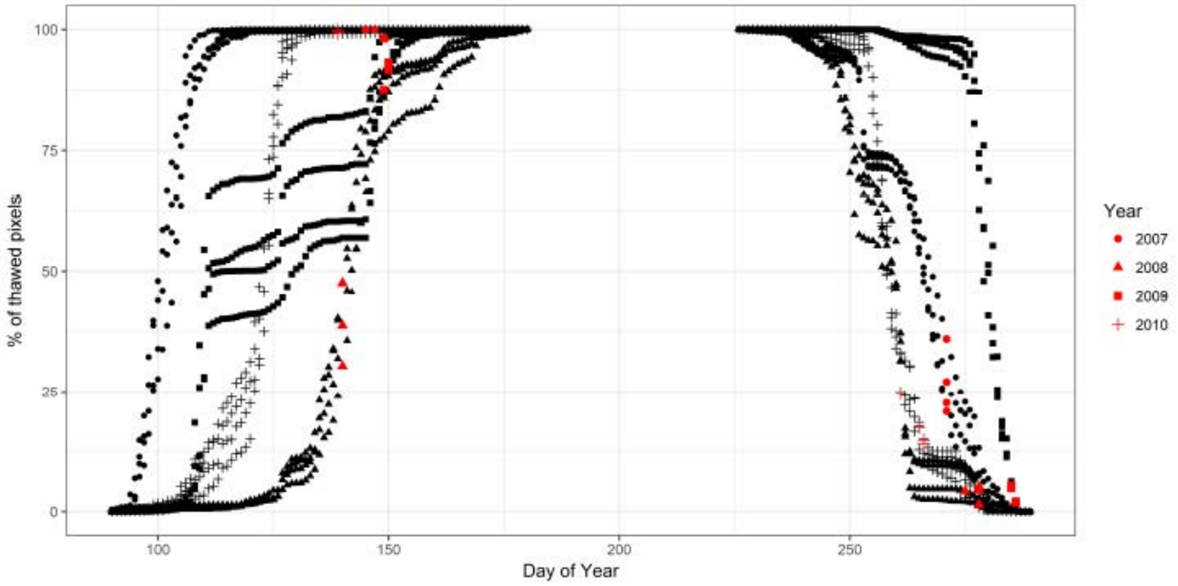

Figure 11. Percentage of thawed SAR pixel within one ASCAT grid cell during transitional periods (indicated by the DOY), including DOY of the last surface state change in the ASCAT product (red symbols) for the selected grid cells with the assigned landscape type Forest (Laptev Sea 6, Laptev Sea 7, Laptev Sea 8, Laptev Sea 9), for the ASCAT [42] and SAR [42] datasets.

Helena Bergstedt, Annett Bartsch: Surface State across Scales; Temporal and Spatial Patterns in Land Surface Freeze/Thaw Dynamics. Geosciences (Switzerland) 08/2017; 7(3):65.

austrian polar research institute

Summary radar

- Allows investigations with higher spatial resolution using SAR, but data availability is the major constrain
- but good SAR records available for C-band
- Continuity currently only ensured for C-band
- High potential for Ku-band, specifically for changes in the snow pack
- Simple threshold methods are usually not sufficient
- Threshold needs to be defined using temperature data from in situ or reanalyses

SSM/I and SSMR

Zhang & Armstrong (2001)

- SSM/I 19-GHz and 37-GHz vertically-polarized T_Bs discriminate frozen ground from unfrozen ground over prairie soils, using the following equation: $(T_B(37V) - T_B(19V))/18 < 0$ and $T_B(37V) < 258.2$ K
- A similar approach is used with the SMMR data using the 18-Ghz and 37-Ghz channels.

Kim et al. (2011): seasonal threshold approach using $T_B(37V)$ at pm, also applied to AMSR-E and AMS2

$$\Delta T_{bp}(x,t) = \frac{(T_{bp}(x,t) - FrozRef(x))}{(ThawRef(x) - FrozRef(x))}$$

$$\Delta T_{bp}(x,t) > T(x,t)$$

$$\Delta T_{bp}(x,t) \leq T(x,t)$$

L Band: SMOS

slide courtesy of K. Rautiainen (FMI)

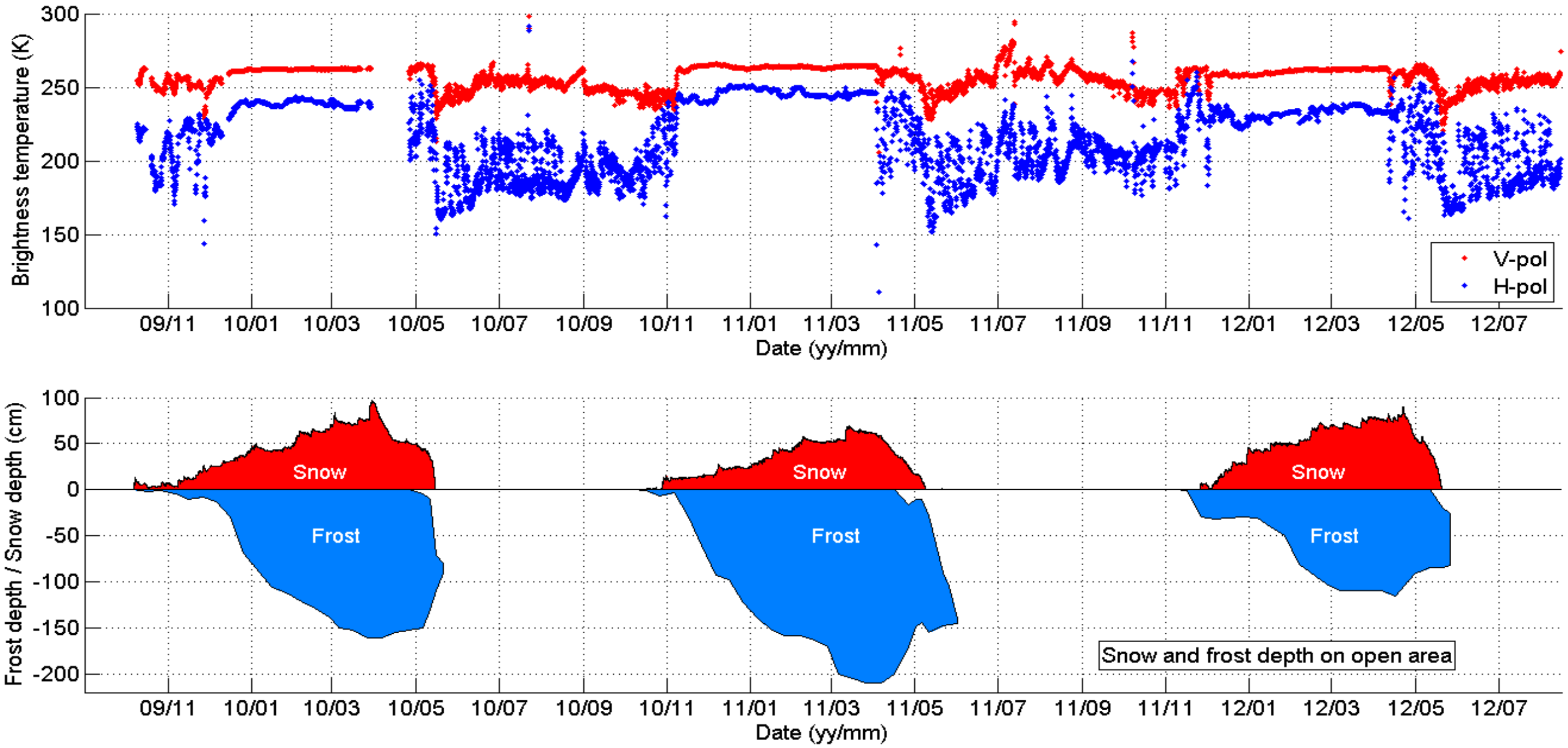

K.Rautiainen, T. Parkkinen, J.Lemmetyinen, M.Schwank, A.Wiesmann, J. Ikonen, C.Derksen, S.Davydov, A. Davydova, J. Boike, M.Langer, M. Drusch, J.Pulliainen (2016): SMOS prototype algorithm for detecting autumn soil freezing. Remote Sensing of Environment 180 (2016) 346–360

L Band: SMOS

slide courtesy of K. Rautiainen (FMI)

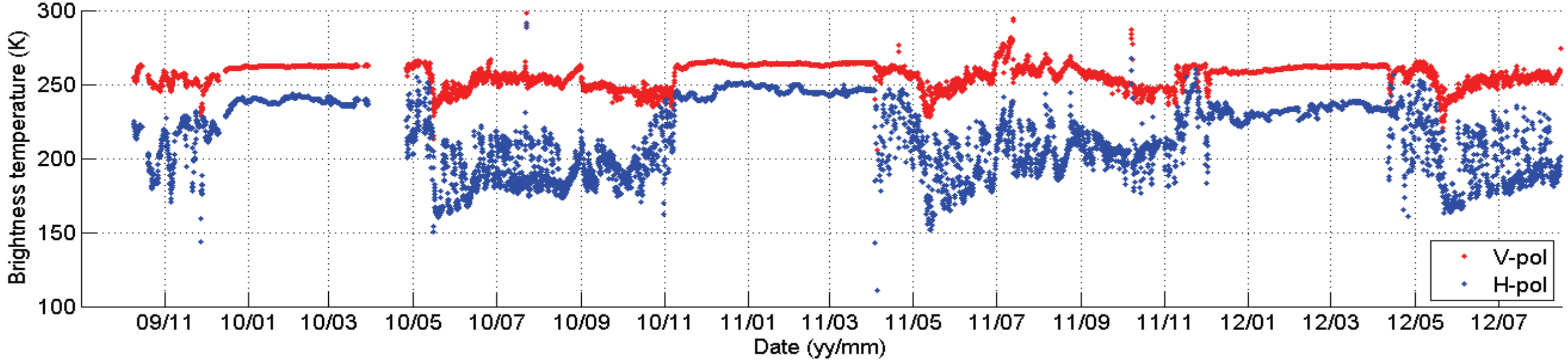

Soil freezing has following effects to L-band passive signal:

- Increased and saturated observed brightness temperature T_B
- Decrease in polarization difference: $T_B^V - T_B^H$

K.Rautiainen, T. Parkkinen, J.Lemmetyinen, M.Schwank, A.Wiesmann, J. Ikonen, C.Derksen, S.Davydov, A. Davydova, J. Boike, M.Langer, M. Drusch, J.Pulliainen (2016): SMOS prototype algorithm for detecting autumn soil freezing. Remote Sensing of Environment 180 (2016) 346–360

L Band: SMOS

slide courtesy of K. Rautiainen (FMI)

NPR - Normalized polarization ratio

- Observed T_B values converted to $FF_{NPR} = \frac{T_B^V - T_B^H}{T_B^V + T_B^H}$
- Pixel-wise freeze and thaw references determined using all available data (one freeze and one thaw reference per pixel)

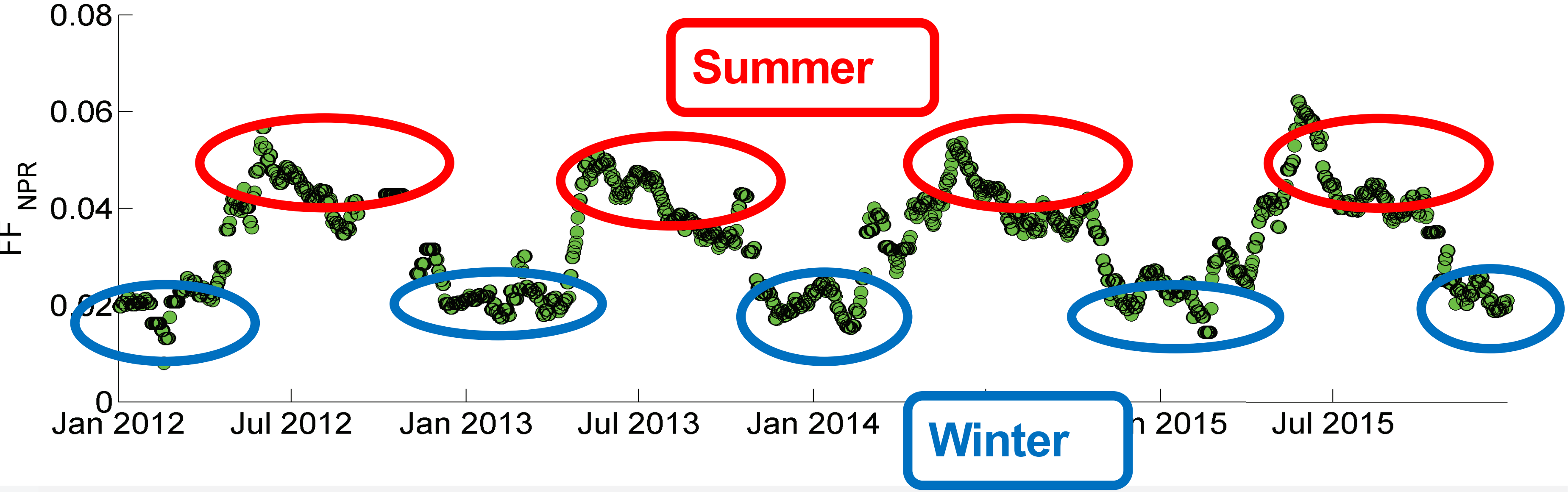

K.Rautiainen, T. Parkkinen, J.Lemmetyinen, M.Schwank, A.Wiesmann, J. Ikonen, C.Derksen, S.Davydov, A. Davydova, J. Boike, M.Langer, M. Drusch, J.Pulliainen (2016): SMOS prototype algorithm for detecting autumn soil freezing. Remote Sensing of Environment 180 (2016) 346–360

L Band: SMOS

slide courtesy of K. Rautiainen (FMI)

Frost depth observation network operated by Finnish Environmental Institute (SYKE)

Pixel-wise FF values compared against observed frost depths

➢ Exponential fit => thresholds defined

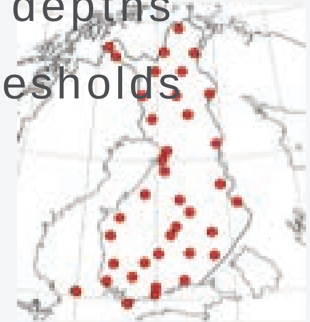

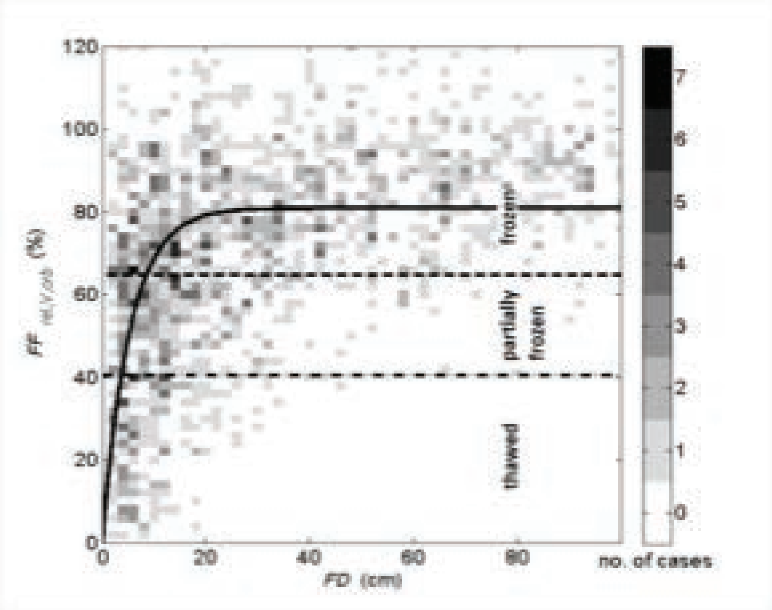

K.Rautiainen, T. Parkkinen, J.Lemmetyinen, M.Schwank, A.Wiesmann, J. Ikonen, C.Derksen, S.Davydov, A. Davydova, J. Boike, M.Langer, M. Drusch, J.Pulliainen (2016): SMOS prototype algorithm for detecting autumn soil freezing. Remote Sensing of Environment 180 (2016) 346–360

L Band: SMAP

- The algorithm uses the normalized polarization ratio (NPR) of SMAP radiometer measurements defined by:

$$NPR=(TBV-TBH)/(TBV+TBH)$$

- A seasonal scale factor D(t) is defined for an observation acquired at time *t* as:

$$Dt=(NPR(t)-NPR(fr))/(NPR(th)-NPR(fr))$$

- where NPR(*t*) is the normalized polarization ratio calculated at time *t*, for which a freeze/thaw classification is sought, and NPR(fr) and NPR(th) are normalized polarization ratios corresponding to the frozen and thawed reference states, respectively. Threshold value is 0.5

C.Derksen, X. Xu, R. S. Dunbar, A. Colliander, Y.Kim, J.S. Kimball, T. A. Black, E.Euskirchen, A. Langlois, M. M. Loranty, P. Marsh, K. Rautiainen, A.Roy, A. Royer, J. Stephens, Retrieving landscape freeze/thaw state from Soil Moisture Active Passive (SMAP) radar and radiometer measurements, Remote Sensing of Environment, Volume 194, 2017, Pages 48-62.

L Band: SMAP

Freeze and thaw references

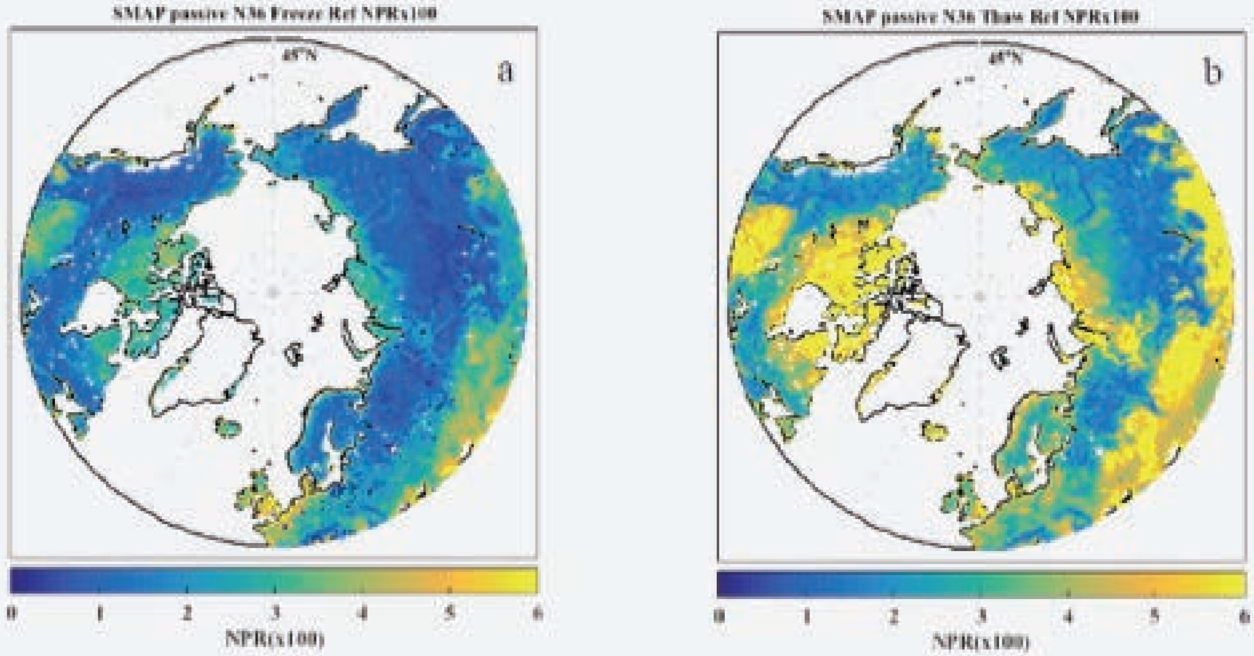

C.Derksen, X. Xu, R. S. Dunbar, A. Colliander, Y.Kim, J.S. Kimball, T. A. Black, E.Euskirchen, A. Langlois, M. M. Loranty, P. Marsh, K. Rautiainen, A.Roy, A. Royer, J. Stephens, Retrieving landscape freeze/thaw state from Soil Moisture Active Passive (SMAP) radar and radiometer measurements, Remote Sensing of Environment, Volume 194, 2017, Pages 48-62.

Summary – passive microwave

- Varying approaches
  - Use of different frequencies
  - Use of different polarizations
  - Summer and winter references used

- Threshold needs to be defined using temperature data from in situ or reanalyses

Validation

- Air temperature
- Snow height
- Soil temperatures – not that many sites, but e.g. permafrost boreholes

- Need to convert continuous values to yes/no information

Validation

WMO and GTN-P borehole data (point versus 25km gridded ASCAT)

Station	Temperature	Agreement with SSF [%]
Nadym R1	surface	91.79
Nadym R1	air	90.36
R3 Marre Sale	0.02m below ground	82.75
R3 Marre Sale	0.5m below ground	80.13
R33 Borehole 3	0m surface	80.36
R33 Borehole 3	0.5m below ground	71.90

ASCAT (METOP-A) SSF
Unfrozen Frozen Unknown Temporary Water on Surface/Snow melt
Precipitaion and SWE (Snow Water Equivalent) data are extracted from GLDAS-NOAH dataset

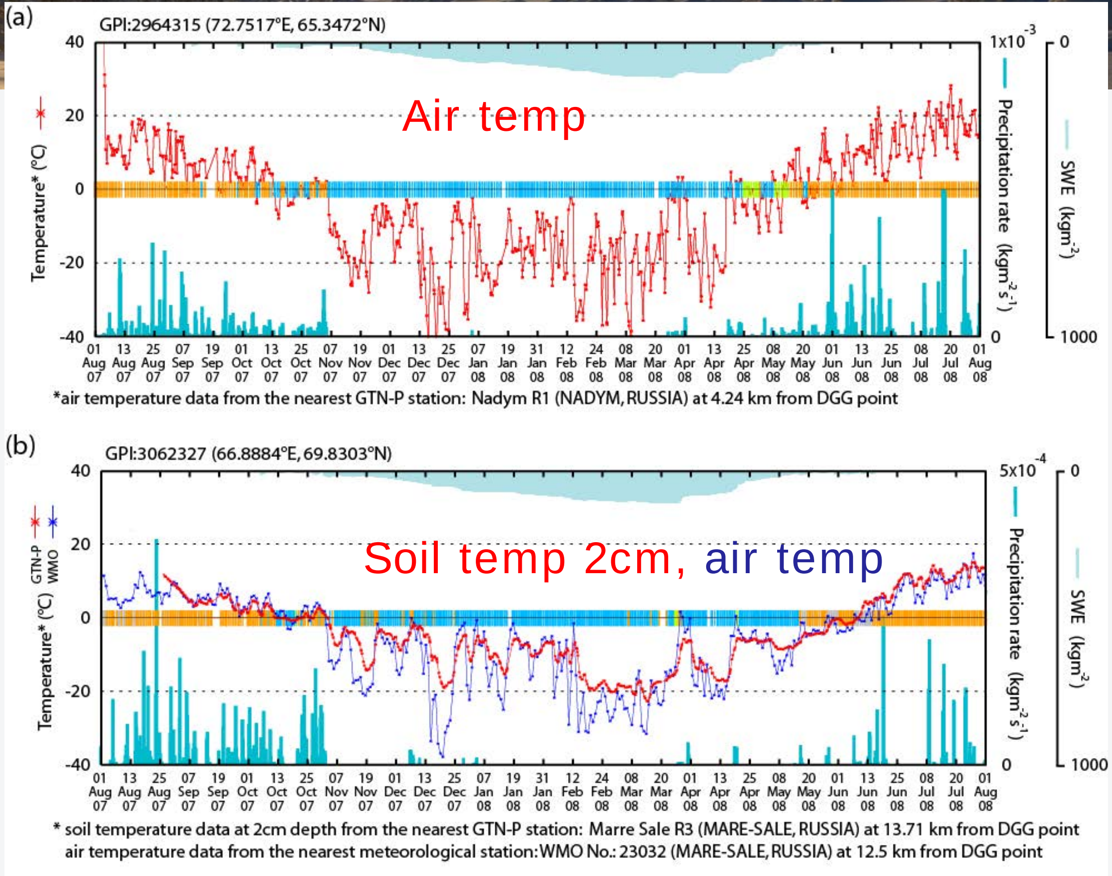

Naeimi, V., Paulik, C., Bartsch, A., Wagner, W., Kidd, R. Park, S.-E., Elger, K., Boike, J. 2012: *ASCAT Surface State Flag (SSF): Extracting Information on Surface Freeze/Thaw Conditions from Backscatter Data Using an Empirical Threshold-Analysis Algorithm*. IEEE TGRS 50(7): 2566

Applications

- Entire Arctic
- Basins
- Locally

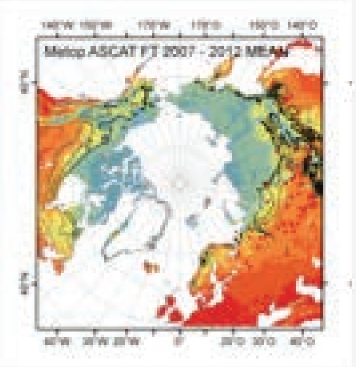

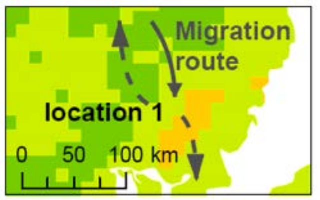

Application – melting snow

Timing of snow melt from diurnal difference Ku-band

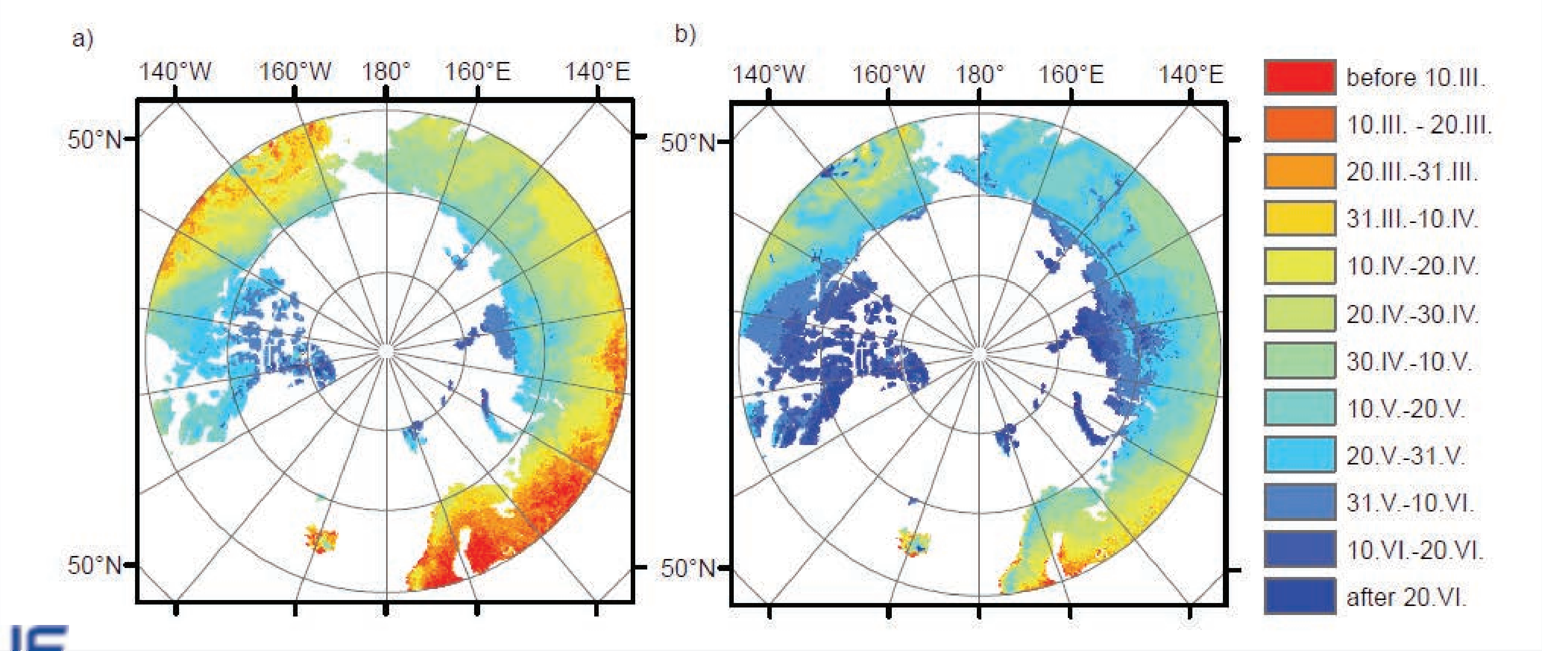

Bartsch, A. 2010: *Ten years of SeaWinds on QuikSCAT for snow applications*. Remote Sensing 04, 2(4).

Application – melting snow

Melt area versus river discharge

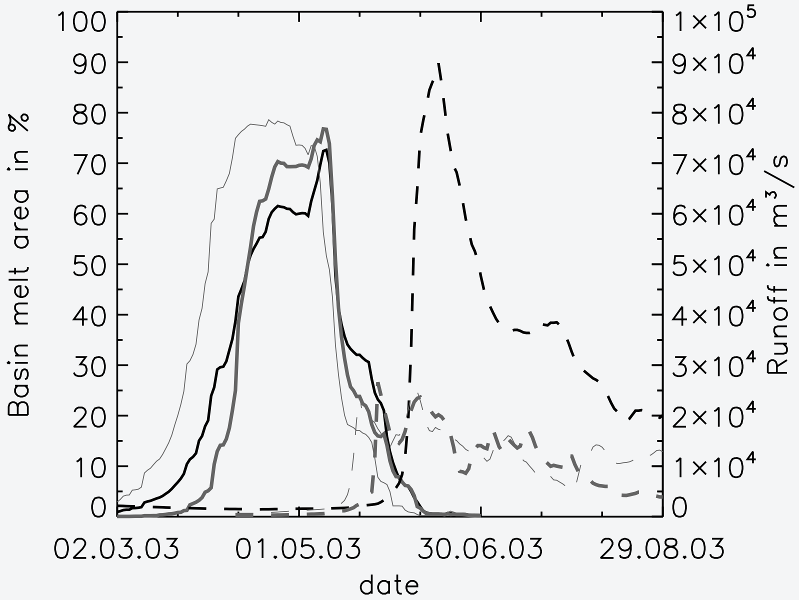

QuikScat derived daily basin melt area in % of the Lena Kyusyur basin (black solid thick line), Uppler Lena Solyanka basin (solid thin grey line), Aldan basin (thick grey solid line) and river discharge in m3/s at corresponding stations (dashed lines)

Bartsch (2010b)

A. Bartsch: Monitoring of Terrestrial Hydrology at High Latitudes with Scatterometer Data. Geoscience and Remote Sensing.New Achievements, 02/2010

Application – melting snow

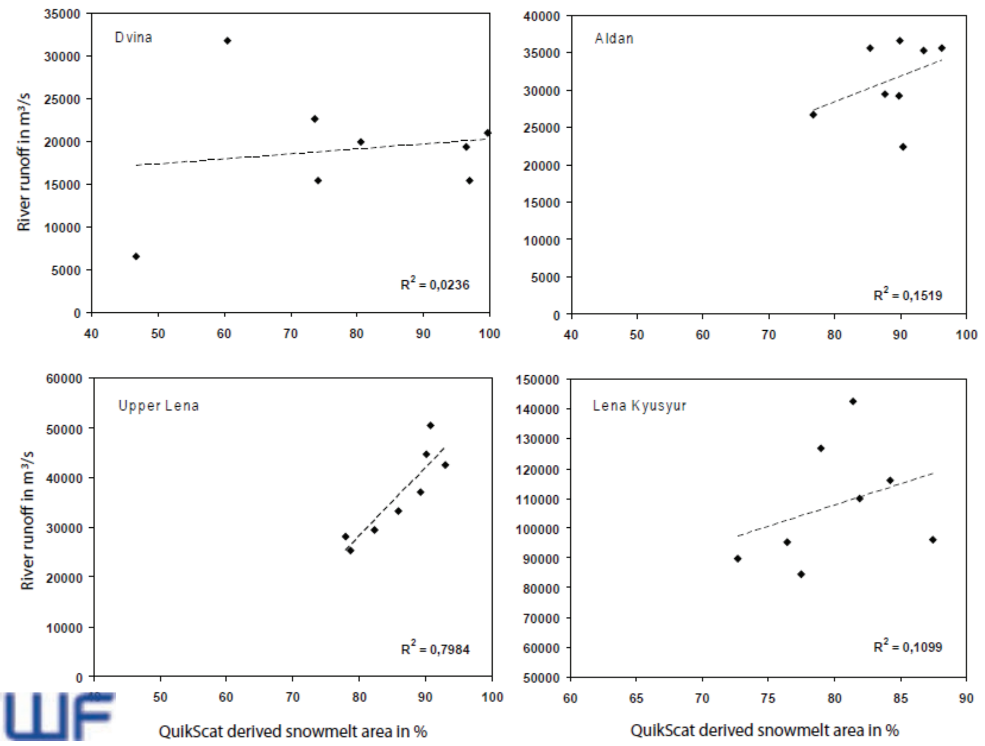

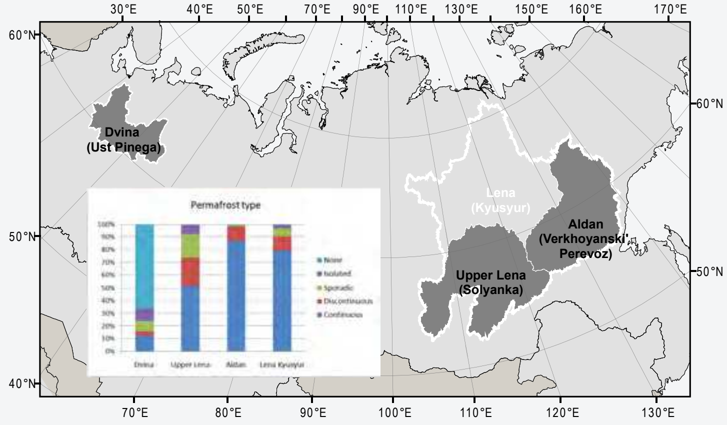

Bartsch (2010b)

A. Bartsch: Monitoring of Terrestrial Hydrology at High Latitudes with Scatterometer Data. Geoscience and Remote Sensing.New Achievements, 02/2010

Ku-band diurnal cycling

Microbial activity starting when snow starts to melt

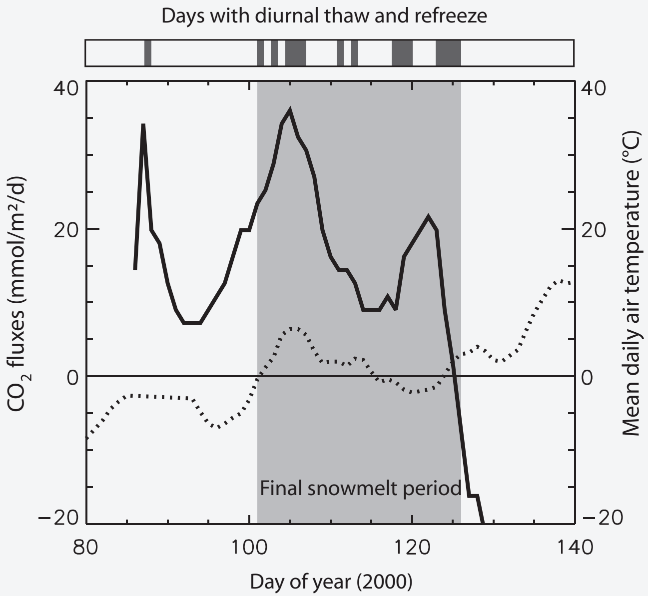

Fig. 9.8 Days with significant backscatter changes due to diurnal thaw and refreeze at Zotino (60.75° N, 89.38° E), smoothed (5 days) spring daily accumulated CO_2 fluxes (*solid line*) and mean daily air temperature (*dashed line*) in 2000 (source: TCOS Siberia). Duration of major and final melt period is indicated by *grey shading*. Adapted from Bartsch et al. (2007)

A. Bartsch, W. Wagner, R. Kidd: Remote Sensing of Spring Snowmelt in Siberia. Environmental Change in Siberia, 01/2010: pages 135-155

Surface state from ASCAT

Globpermafrost WebGIS

www.globpermafrost.info

Number of frozen days

http://maps.awi.de/map/map.html?cu=globpermafrost_arctic&sb=e&zm=1&ctr=[69.78107758124735,-97.23345073130245]&lyr=["globpermafrost-arctic::GTNP WMO Thermal State of Permafrost TSP","globpermafrost-arctic::GTNP WMO Circumpolar Active Layer Moinitoring CALM","globpermafrost-arctic::EU-INTERACT Research and Monitoring Stations","globpermafrost-arctic::International Arctic Research and Monitoring Networks","globpermafrost-arctic::Average Number of Frozen Days per Year from Metop ASCAT 2007-2012"]#mapcontent

ASCAT Surface state and ground temperatures

Number of frozen days

Mean Annual Ground temperature

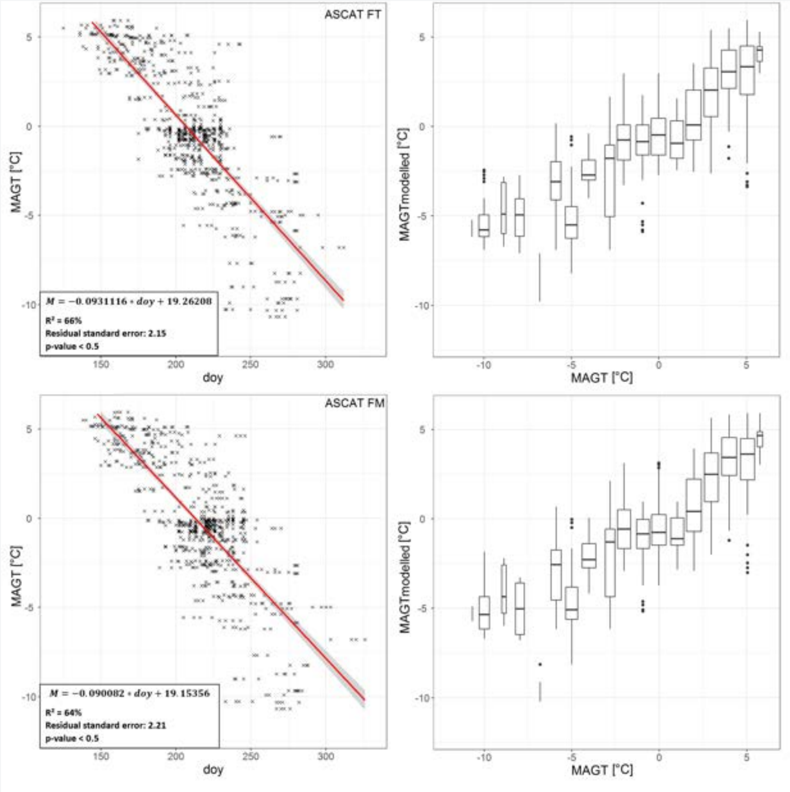

Melting snow as frozen soil

$R^2 = 0.64$

Melting snow as thawing soil

$R^2 = 0.66$

Kroisleitner, C., Bartsch, A., and Bergstedt, H.: Potential permafrost distribution and ground temperatures based on surface state obtained from microwave satellite data, The Cryosphere Discuss., https://doi.org/10.5194/tc-2017-162, in review, 2017.

austrian polar research institute

ASCAT Surface state and groun

Temperatures from lineat fit

Neglects snow and soil properties

Black lines are permafrost zones
(source: Brown et al. 1997)

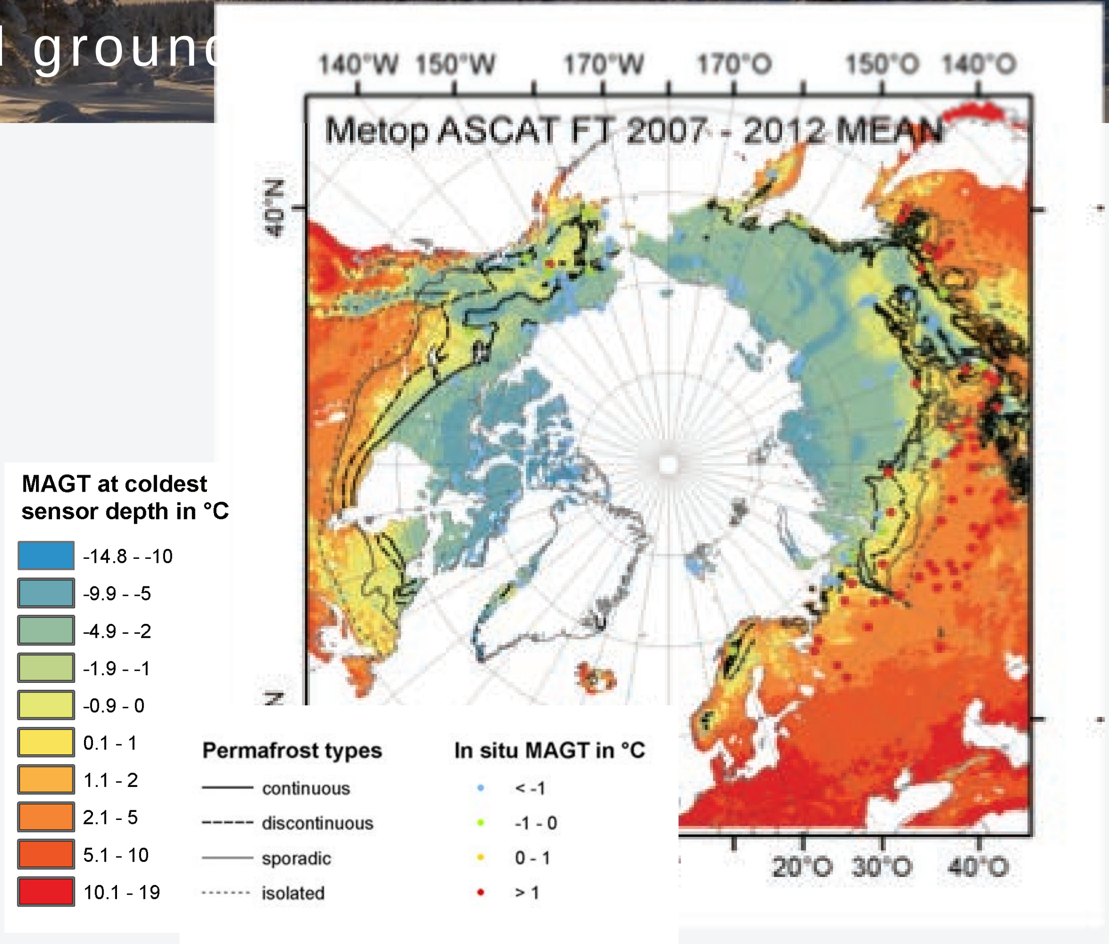

Kroisleitner, C., Bartsch, A., and Bergstedt, H.: Potential permafrost distribution and ground temperatures based on surface state obtained from microwave satellite data, The Cryosphere Discuss., https://doi.org/10.5194/tc-2017-162, in review, 2017.

QuikScat Rain-on-Snow

A. Bartsch, et al. 2010

- Southern Yamal peninsula has been affected by a rain-on-snow (ROS) event in November 2006.
- The ROS event and subsequent refreezing with formation of ice crusts forced a major change in migration.
- Some of the brigades were additionally affected by an event to the west in January and as they migrated back northwards across the snowpack, which still consisted of the previous ice layers. The loss amounted to 25% of the animals including deaths and still-births resulting from exhaustion and poor nutrition of pregnant females.

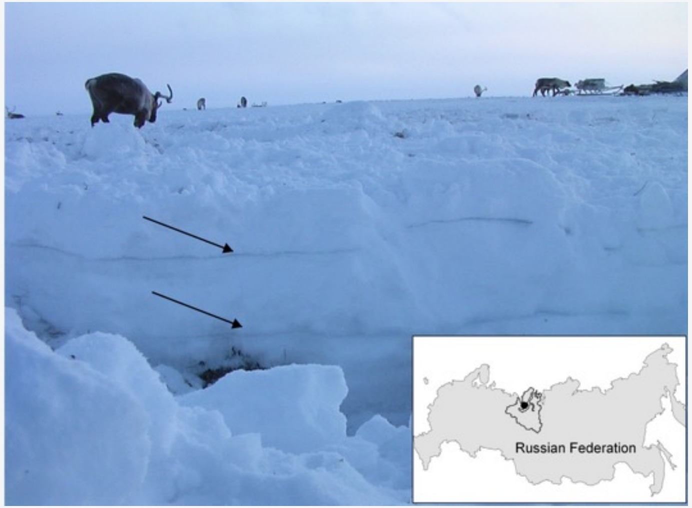

Snow profile taken on the 19th of November 2006. (Photo: Florian Stammler)

Annett Bartsch, Timo Kumpula, Bruce C Forbes, Florian Stammler: Detection of Snow Surface Thawing and Refreezing in the Eurasian Arctic Using QuikSCAT:Iimplications for Reindeer Herding. Ecological Applications 12/2010; 20(8):2346-58.

QuikScat Rain-on-Snow

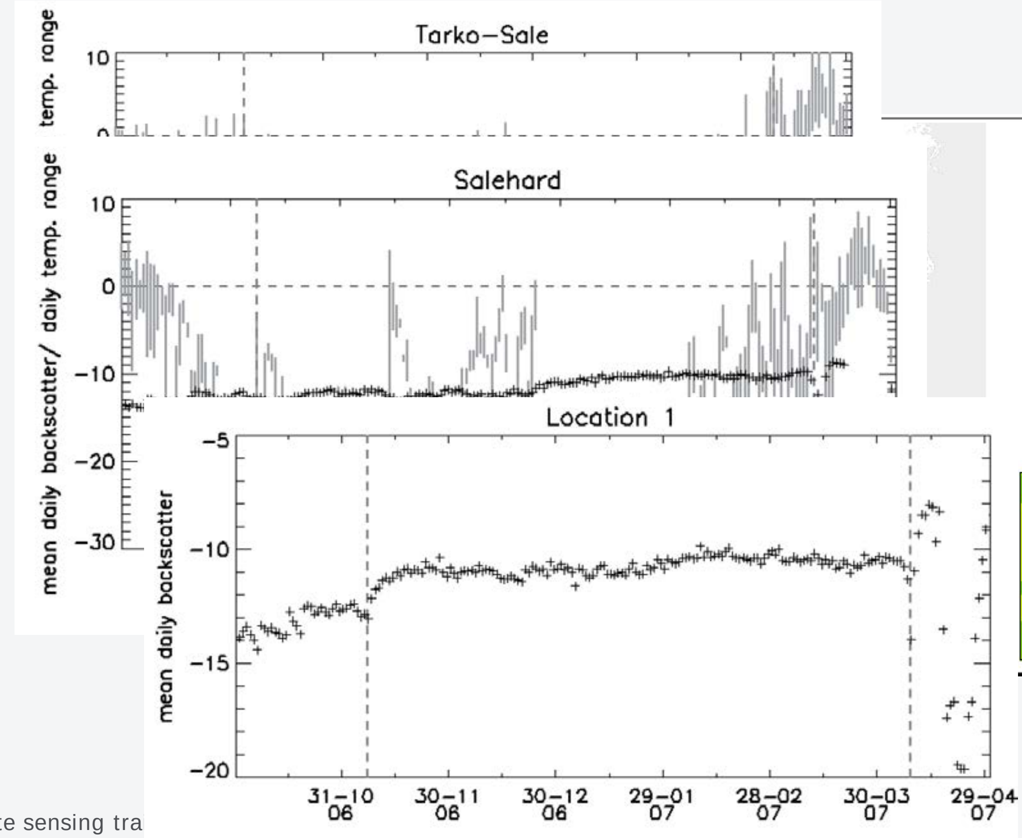

A. Bartsch, et al. 2010

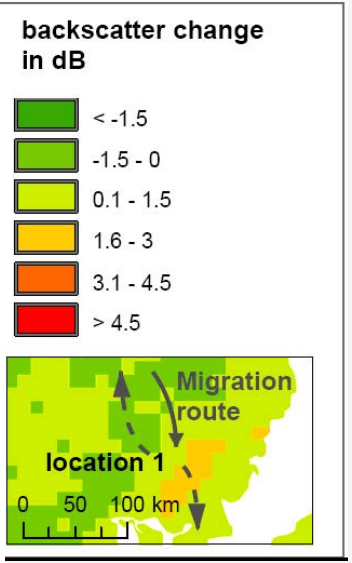

Annett Bartsch, Timo Kumpula, Bruce ... in the Eurasian Arctic Using QuikSCAT:implications for Reindeer Herding. Ecological Applications 12/2010; 20(8):2346-58.

QuikScat Rain-on-Snow

- Comparison with WMO station data

A. Bartsch, et al. 2010

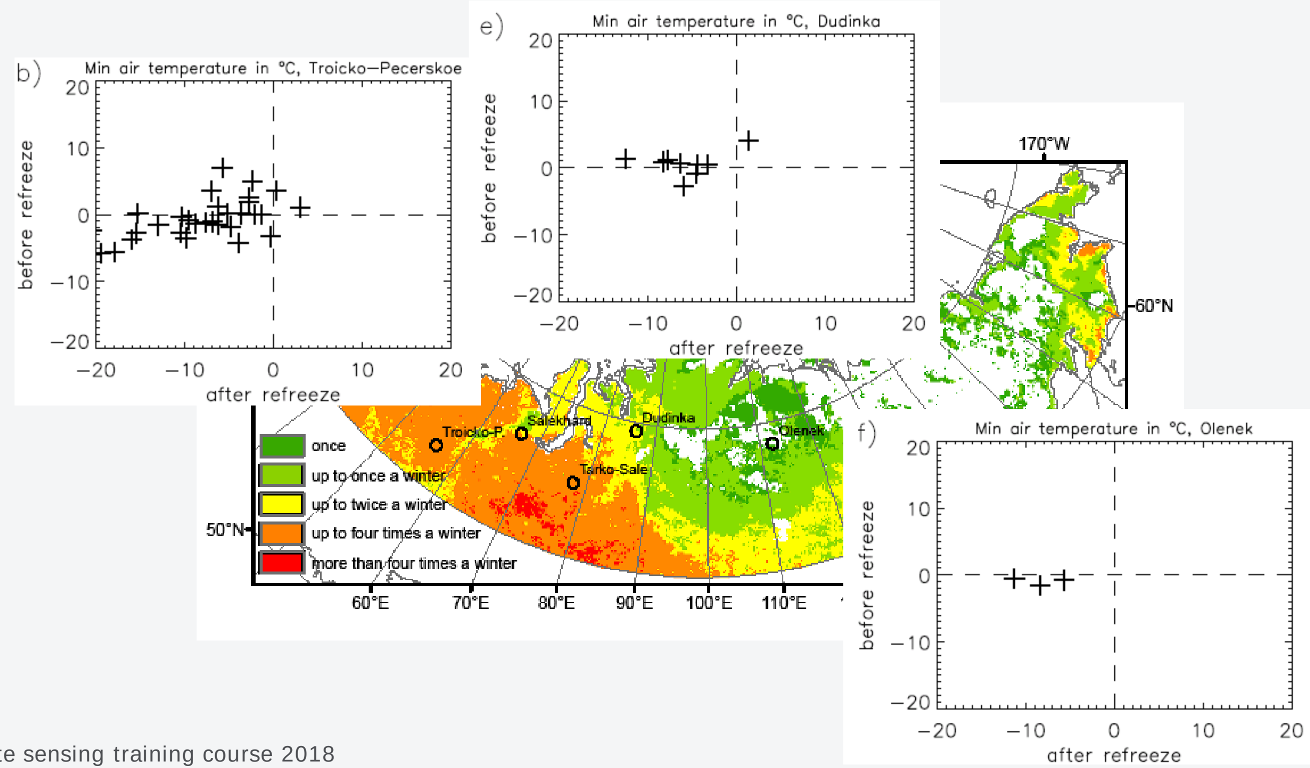

Annett Bartsch, Timo Kumpula, Bruce C Forbes, Florian Stammler: Detection of Snow Surface Thawing and Refreezing in the Eurasian Arctic Using QuikSCAT:Implications for Reindeer Herding. Ecological Applications 12/2010; 20(8):2346-58.

QuikScat Rain-on-Snow

A. Bartsch, et al. 2010

- Increase of snow depth in a very short time?

- Snow structure change

Meteorological records Russia (WMO512)

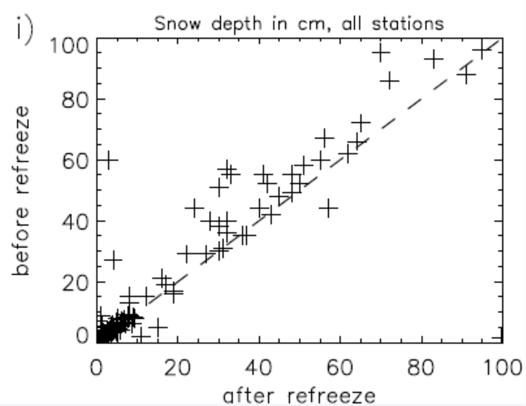

Annett Bartsch, Timo Kumpula, Bruce C Forbes, Florian Stammler: Detection of Snow Surface Thawing and Refreezing in the Eurasian Arctic Using QuikSCAT:Iimplications for Reindeer Herding. Ecological Applications 12/2010; 20(8):2346-58.

ASCAT Rain-on-Snow and Sea Ice

- Evidence for autumn atmospheric warming and precipitation increases over Arctic coastal lands in proximity to Barents and Kara sea ice loss.

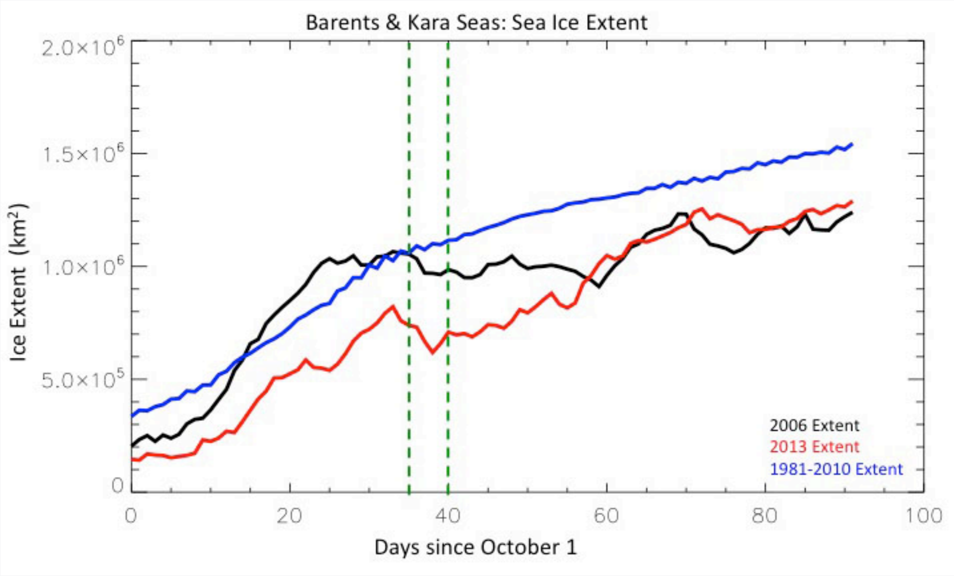

Source: SSMI derived sea ice extent on NSIDC

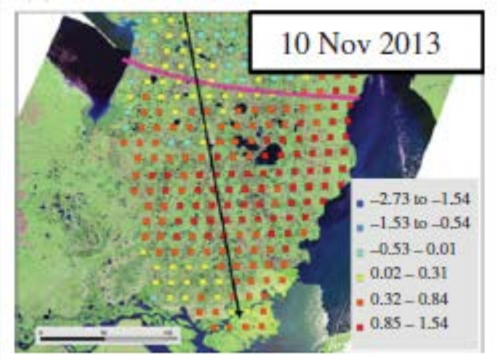

ASCAT backscatter change in dB

Bruce C. Forbes, Timo Kumpula, Nina Meschtyb, Roza Laptander, Marc Macias-Fauria, Pentti Zetterberg, Mariana Verdonen, Anna Skarin, Kwang-Yul Kim, Linette N. Boisvert, Julienne C. Stroeve, Annett Bartsch: Sea ice, rain-on-snow and tundra reindeer nomadism in Arctic Russia. Biology letters 11/2016; 12(11):20160466

QuikScat Rain-on-Snow

Change detection, short term increase of backscatter

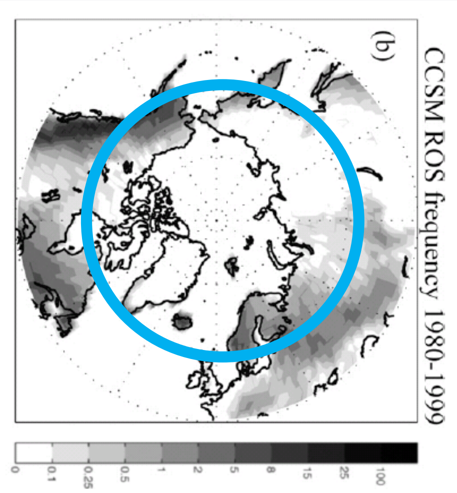

0 125

Rennert et al. 2009

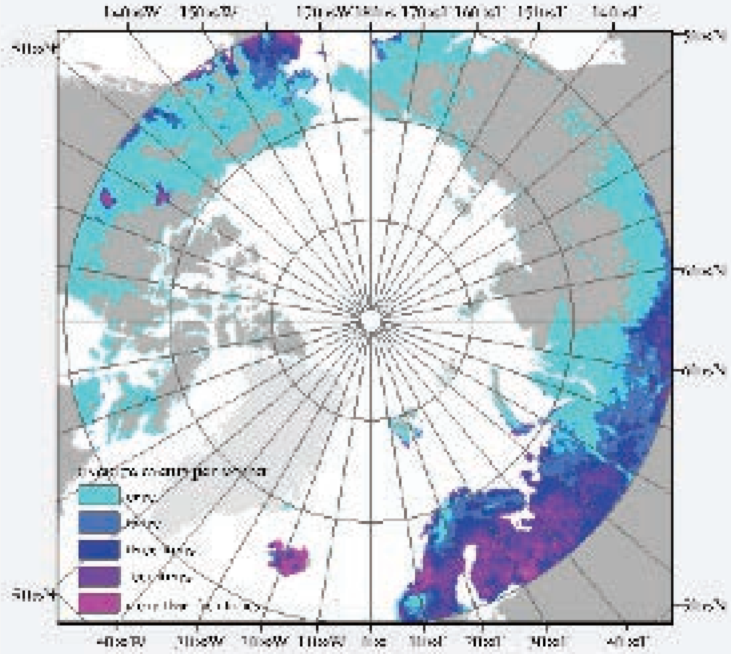

Nov.-Feb. 2000-2009

Bartsch (2010): Ten years of SeaWinds on QuikSCAT for snow applications *Remote Sensing.*

QuikScat Snow structure change

Impacts for Caribou

Western Alaska

Landscape Conservation

Cooperative.

Average number of events

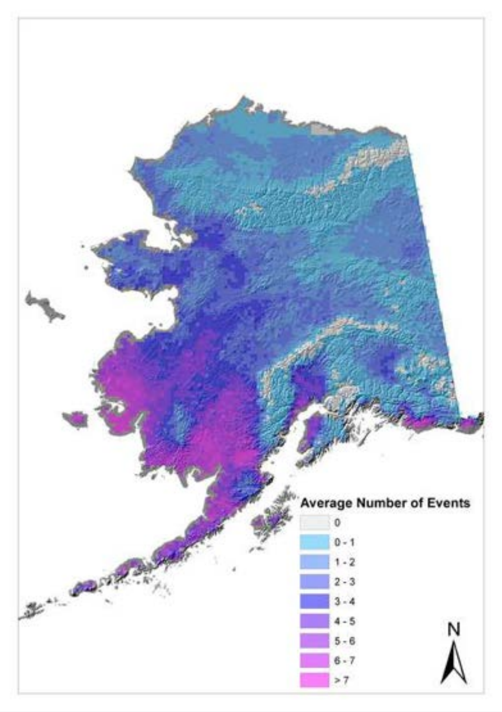

Average size of events

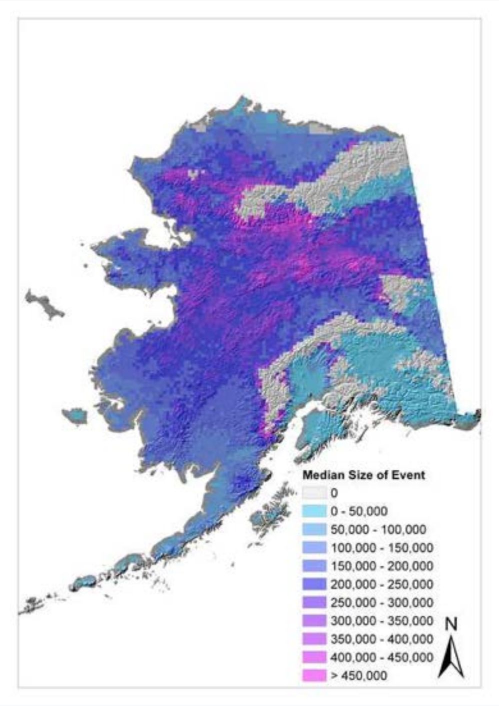

Median 470 km²

Wilson, R.R., Bartsch A, Joly, K., Reynolds, J.H., Orlando, A., Loya, W.M. (2013): Frequency, timing, extent, and size of winter thaw-refreeze events in Alaska 2001-2008 detected by remotely sensed microwave backscatter data. Polar Biology

QuikScat Snow structure change

Yukon basin

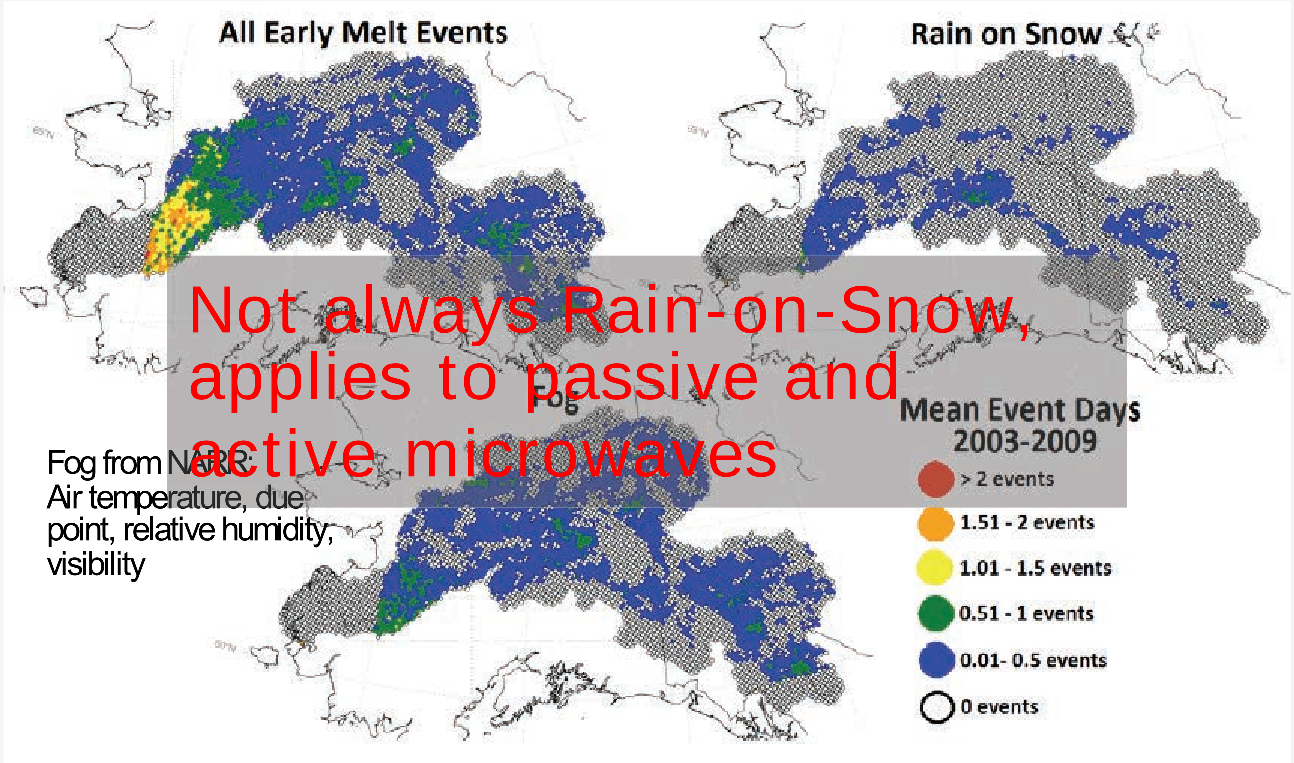

Fog from NARR:
Air temperature, due point, relative humidity, visibility

Not always Rain-on-Snow, applies to passive and active microwaves

K. A. Semmens, J. Ramage, A. Bartsch, and G. E. Liston (2013). Early snowmelt events: detection, distribution, and significance in a major sub-arctic watershed. *Environmental Research Letters*

Rain-on-Snow

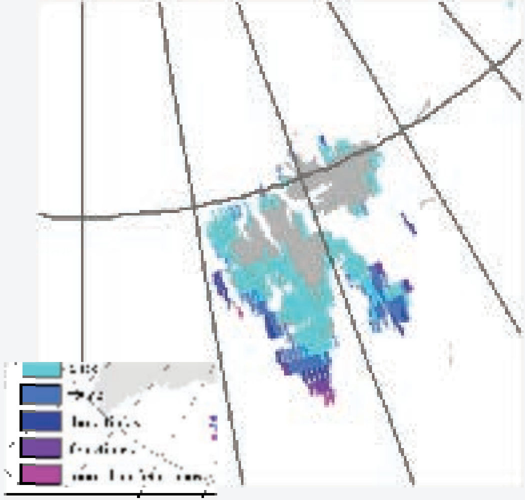

Nov.-Feb. 2000-2009

Bartsch (2010): Ten years of SeaWinds on QuikSCAT for snow applications *Remote Sensing.*

The extreme warm spell and ROS events in January–February 2012 had major implications for the society and wildlife in Svalbard.

(a) Slush avalanches caused closed roads and schools and destroyed a bridge in the major settlement Longyearbyen (photo: Kjersti Strømmen).

(b) A thick layer of ground-ice built up on roads and airport runways in Longyearbyen (photo: Øystein Varpe) and Ny-Ålesund.

(c) A wild female reindeer struggles to find food on the ice-encapsulated tundra in Reindalen one week subsequent to the warm spell and ROS (photo: Brage B Hansen).

Hansen et al. 2014: Warmer and wetter winters: characteristics and implications of an extreme weather event in the High Arctic. ERL

Rain-on-Snow

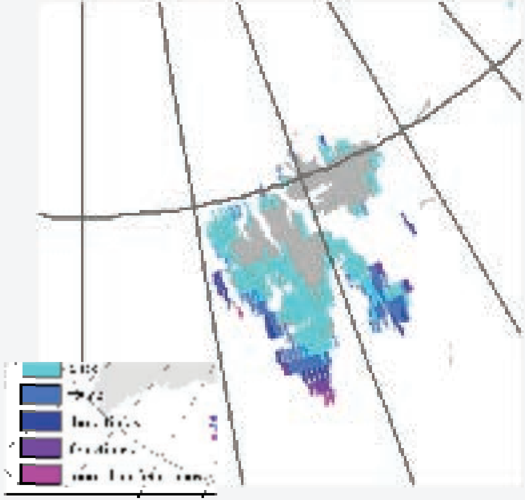

Wild Svalbard reindeer (*Rangifer tarandus platyrhynchus*), the Svalbard rock ptarmigan (*Lagopus muta hyperborea*), and the sibling vole (*Microtus levis*), and one shared consumer, the arctic fox (*Vulpes lagopus*).
The community's population fluctuations are mainly driven by rain-on-snow events

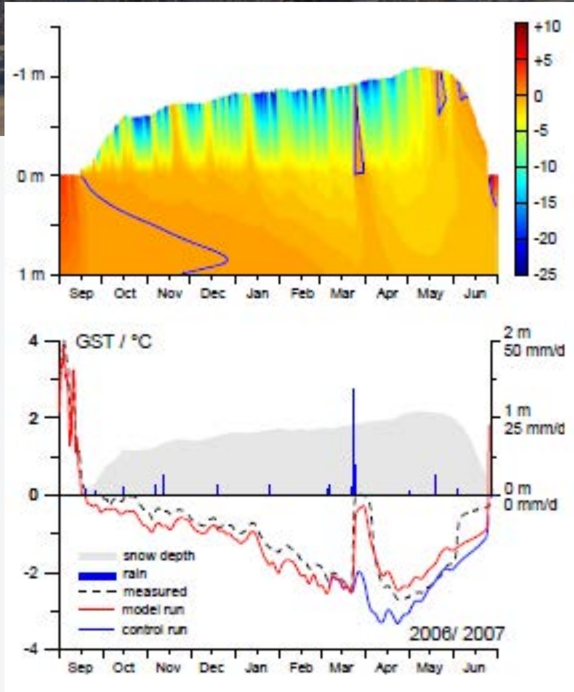

Nov.-Feb. 2000-2009

Bartsch (2010): Ten years of SeaWinds on QuikSCAT for snow applications *Remote Sensing.*

Hansen, B.B; V. Grøtan, R. Aanes, B.-E. Sæther, A. Stien, E. Fuglei, R.A. Ims, N.G. Yoccoz, A.Ø. Pedersen. Climate Events Synchronize the Dynamics of a Resident Vertebrate Community in the High Arctic. Science, 18 Jan. 2013

Westermann, S., Boike, J., Langer, M., Schuler, T. V., and Etzelmüller, B.: Modeling the impact of wintertime rain events on the thermal regime of permafrost, The Cryosphere, 5, 945-959, https://doi.org/10.5194/tc-5-945-2011, 2011.

Summary freeze/thaw

- Monitoring of landsurface
  - Changes type throughout the season: We need to consider snow and/or soils

- Relevant for e.g.
  - Soil processes, e.g. microbial activity → carbon cycle
  - Snow properties of relevance for subsoil temperatures → permafrost
  - Changes in snow structure → wild life

List of references I

Bartsch, A., Kidd, R., Wagner, W. and Z. Bartalis (2007): Temporal and spatial variability of the beginning and end of daily spring freeze/thaw cycles derived from scatterometer data. Remote Sensing of Environment, 106(3), 360-374, doi:10.1016/j.rse.2006.09.004

Bartsch, A, W Wagner, K Scipal, C Pathe, D Sabel, P Wolski (2009): Global monitoring of wetlands — the value of ENVISAT ASAR global mode. Journal of Environmental Management 90(7):2226-33., DOI:10.1016/j.jenvman.2007.06.023

Bartsch, A, Timo Kumpula, Bruce C Forbes, Florian Stammler: Detection of Snow Surface Thawing and Refreezing in the Eurasian Arctic Using QuikSCAT:Iimplications for Reindeer Herding. Ecological Applications 12/2010; 20(8):2346-58., DOI:10.1890/09-1927

Bartsch, A: Ten years of SeaWinds on QuikSCAT for snow applications. Remote Sensing 04/2010; 2(4)., DOI:10.3390/rs2041142

Bartsch, A: Monitoring of Terrestrial Hydrology at High Latitudes with Scatterometer Data. Geoscience and Remote Sensing New Achievements, 02/2010; , ISBN: 978-953-7619-97-8, DOI:10.5772/9095

Bartsch, A. & W. Wagner, R. Kidd: Remote Sensing of Spring Snowmelt in Siberia. Environmental Change in Siberia, 01/2010: pages 135-155

Helena Bergstedt, Simon Zwieback, Annett Bartsch, Marina Leibman: Dependence of C-Band Backscatter on Ground Temperature, Air Temperature and Snow Depth in Arctic Permafrost Regions. Remote Sensing 01/2018; 10(1)., DOI:10.3390/rs10010142

Helena Bergstedt, Annett Bartsch: Surface State across Scales; Temporal and Spatial Patterns in Land Surface Freeze/Thaw Dynamics. Geosciences (Switzerland) 08/2017; 7(3):65., DOI:10.3390/geosciences7030065

Chris Derksen, Xiaolan Xu, R. Scott Dunbar, Andreas Colliander, Youngwook Kim, John S. Kimball, T. Andrew Black, Eugenie Euskirchen, Alexandre Langlois, Michael M. Loranty, Philip Marsh, Kimmo Rautiainen, Alexandre Roy, Alain Royer, Jilmarie Stephens, Retrieving landscape freeze/thaw state from Soil Moisture Active Passive (SMAP) radar and radiometer measurements, Remote Sensing of Environment, Volume 194, 2017, Pages 48-62.

Bruce C. Forbes, Timo Kumpula, Nina Meschtyb, Roza Laptander, Marc Macias-Fauria, Pentti Zetterberg, Mariana Verdonen, Anna Skarin, Kwang-Yul Kim, Linette N. Boisvert, Julienne C. Stroeve, Annett Bartsch: Sea ice, rain-on-snow and tundra reindeer nomadism in Arctic Russia. Biology letters 11/2016; 12(11):20160466., DOI:10.1098/rsbl.2016.0466

List of references II

Vahid Naeimi, Christoph Paulik, Annett Bartsch, Wolfgang Wagner, Richard Kidd, Sang-Eun Park, Kirsten Elger, Julia Boike: ASCAT Surface State Flag (SSF): Extracting Information on Surface Freeze/Thaw Conditions from Backscatter Data Using an Empirical Threshold-Analysis Algorithm. IEEE Transactions on Geoscience and Remote Sensing 07/2012; 50(7):2566-2582., DOI:10.1109/TGRS.2011.2177667

Kim, Youngwook, John S Kimball, Kyle C McDonald, and Joseph Glassy. 2011. 'Developing a global data record of daily landscape freeze/thaw status using satellite passive microwave remote sensing', Geoscience and Remote Sensing, IEEE Transactions on, 49: 949-60.

Sang-Eun Park, Annett Bartsch, Daniel Sabel, Wolfgang Wagner, Vahid Naeimi, Yoshio Yamaguchi: Monitoring freeze/thaw cycles using ENVISAT ASAR Global Mode. Remote Sensing of Environment 12/2011; 115(12)., DOI:10.1016/j.rse.2011.08.009

C. Paulik, A. Bartsch, D. Sabel, W. Wagner, C. Duguay, A. Soliman: Intercomparison of active microwave derived surface status and MODIS land surface temperature at high latitudes. Proceedings of 2012 IEEE International Geoscience & Remote Sensing Symposium; 07/2012, DOI:10.1109/IGARSS.2012.6350444

Kimmo Rautiainen, Tiina Parkkinen, Juha Lemmetyinen, Mike Schwank, Andreas Wiesmann, Jaakko Ikonen, Chris Derksen, Sergei Davydov, Anna Davydova, Julia Boike, Moritz Langer, Matthias Drusch, Jouni Pulliainen (2016): SMOS prototype algorithm for detecting autumn soil freezing. Remote Sensing of Environment 180 (2016) 346–360

Kathryn Alese Semmens, Joan Ramage, Annett Bartsch, Glen E Liston: Early snowmelt events: Detection, distribution, and significance in major sub-arctic watershed. Environmental Research Letters 02/2013; 8(1)., DOI:10.1088/1748-9326/8/1/014020

Anna Maria Trofaier, Sebastian Westermann, Annett Bartsch: Progress in space-borne studies of permafrost for climate science: Towards a multi-ECV approach. Remote Sensing of Environment 06/2017;, DOI:10.1016/j.rse.2017.05.021

F.T. Ulaby and D.G. Long. Microwave radar and radiometric remote sensing. Ann Arbor, University of Michigan Press, 2015

Ryan R. Wilson, Annett Bartsch, Kyle Joly, Joel H. Reynolds, Anne Orlando, Wendy M. Loya: Frequency, timing, extent, and size of winter thaw-refreeze events in Alaska 2001–2008 detected by remotely sensed microwave backscatter data. Polar Biology 03/2013; 36(3):419-426., DOI:10.1007/s00300-012-1272

Zhang, T., and R.L. Armstrong. 2001. Soil freeze/thaw cycles over snow-free land detected by passive microwave remote sensing. Geophysical Research Letters 28(5): 763-766.